

An Investigation into Efficiency Improvement of Thin Film Solar Cell

by

Khan Md Arifur Rahman: 200716014

Salman Hasan: 200716019

Md Jannatul Ferdous: 200816043

BACHELOR OF SCIENCE IN ELECTRICAL ELECTRONIC AND COMMUNICATION ENGINEERING



**DEPARTMENT OF ELECTRICAL ELECTRONIC AND COMMUNICATION
ENGINEERING**

**MILITARY INSTITUTE OF SCIENCE AND TECHNOLOGY, DHAKA,
BANGLADESH
December, 2011**

An Investigation into Efficiency Improvement of Thin Film Solar Cell

A thesis submitted to the Department of Electrical, Electronic and Communication
Engineering
MIST
in partial fulfillment of the requirements
for the degree of
**BACHELOR OF SCIENCE IN ELECTRICAL, ELECTRONIC AND COMMUNICATION
ENGINEERING**

by
Khan Md Arifur Rahman (200716014)
Salman Hasan (200716019)
Md Jannatul Ferdous (200816043)



**DEPARTMENT OF ELECTRICAL, ELECTRONIC AND COMMUNICATION
ENGINEERING (EECE)
MILITARY INSTITUTE OF SCIENCE AND TECHNOLOGY, DHAKA,
BANGLADESH
December, 2011**

Supervised by

Yeasir Arafat
Assistant Professor
Department of Electrical, Electronic and Communication Engineering
BUET, Dhaka-1000, Bangladesh

CERTIFICATION OF APPROVAL

The thesis titled “An Investigation into Efficiency Improvement of Thin Film Solar Cell” submitted by Khan Md Arifur Rahman (200716014), Salman Hasan (200716019), Md Jannatul Ferdous (200816043), has been accepted as satisfactory in partial fulfillment of the requirements for the degree of BACHELOR OF SCIENCE IN ELECTRICAL, ELECTRONIC AND COMMUNICATION ENGINEERING on 13 December, 2011.

APPROVAL OF THE SUPERVISOR

Yeasir Arafat

Assistant Professor

Department of Electrical, Electronic and Communication Engineering

BUET, Dhaka-1000, Bangladesh

DECLARATION

It is hereby declared that this thesis or any part of it has not been submitted elsewhere for the award of any degree or diploma.

Authors

(Khan Md Arifur Rahman)
Student No: 200716014

(Salman Hasan)
Student No: 200716019

(Md Jannatul Ferdous)
Student No: 200816043

ABSTRACT

An Investigation into Efficiency Improvement of Thin Film Solar Cell

Thin film solar cell has the potential to be an important contributor to the global energy demand by mid 21st century. Thin film solar cell which has achieved the laboratory efficiency close to 20%, are highly attractive because their band gap is near the optimal value, their polycrystallinity is not significantly detrimental to their performance and the broad choice of heterojunction partners available allows additional degrees of freedom for optimizing their performance. This thesis is intended to improve the efficiency of thin film solar cell by investigating the properties which is related to it. The level of complexity involved is largely prohibitive to analytical treatment and hence numerical approaches are primarily utilized. The optimization is performed in MATLAB along with some other software like ORIGIN, WINDIG etc.

For modeling of a solar cell, we have studied on how to model a heterojunction thin film solar cell for better efficiency. In previous fabrication process, solar cell is fabricated based on homojunction but relatively little attention was paid on the heterojunction thin film solar cell. But as heterojunction opposed the homojunction by creating different bandgap energy level inside the semiconductor, so the performance of the photovoltaic devices also changes. With the passage of time thin film heterojunction solar cell have drawn the attention of researchers by providing higher efficiency. We used CIGS and ZnTeO thin film solar cell for modeling. Rather than other model we have followed one diode model where different parameters are considered related to the performance of solar cell. For evaluating the efficiency of the solar cell, parameter like transmittance, energy bandgap, carrier recombination life time, temperature etc are very important. From our study we have tried to find the relationship between all of these parameters. We have simulated some curve in which the relationship between the above discussed parameter can clearly be identified. Not only that, we can also find the optimal point for all parameters at which the efficiency gets its max value. From our result, we have found that in every case each parameter bears a certain value at which the module performance gets better. So for designing solar cell module, a designer can take a help from this overview.

ACKNOWLEDGEMENTS

Thanks to most merciful, the most gracious and the most cordial, the Almighty Allah at first.

We would like to express our heartiest gratitude and profound respect to our thesis supervisor Yeasir Arafat, Assistant Professor, Department of Electrical and Electronic Engineering (EEE), Bangladesh University of Engineering and Technology (BUET), for giving us the opportunity to work with him and for his continuous guidance, suggestion, inspiration and wholehearted supervision throughout the progress of this work. We are indebted to him for acquainting us with the word of advance research.

We are also giving thanks to our department and Cdr Mahbubur Rahman, Head of the department of Electrical, Electronic and Communication Engineering (EECE), Military Institute of Science and Technology (MIST) for his all time support, co-operation, valuable suggestion and encouragement for completion of this thesis.

MIST, Dhaka
13 December, 2011

Khan Md Arifur Rahman
Salman Hasan
Md Jannatul Ferdous

TABLE OF CONTENTS

DECLARATION	iii
ABSTRACT	iv
ACKNOWLEDGEMENTS	v
LIST OF FIGURES	xi

CHAPTER 1: INTRODUCTION

1.1	General	1
1.2	Solar Cell History	3
1.2.1	First practical cell	4
1.2.2	Berman's price reductions	4
1.2.3	Further improvements	6
1.3	Scope/objective	6
1.4	Structure of the Thesis	7

CHAPTER 2 : THEORY AND APPLICATION OF SOLAR CELL

2.1	Theory of solar cell	8
2.1.1	Simple explanation	9
2.1.2	Photo generation of charge carriers	9
2.1.3	Charge carrier separation	10
2.1.4	The p-n junction	11
2.1.5	Equivalent circuit of a solar cell	12
2.1.6	One-Diode Model	14
2.1.7	Characteristic equation	15
2.1.8	Open-circuit voltage and short-circuit current	17
2.1.9	Effect of physical size	18

2.1.10	Cell temperature	19
2.1.11	Resistance	21
2.1.11.1	Series resistance	21
2.1.11.2	Shunt resistance	22
2.1.12	Reverse saturation current	23
2.1.13	Transmittance	24
2.1.14	Ideality factor	24
2.2	Applications	26
2.2.1	Standalone systems	26
2.2.2	Solar vehicles	28
2.2.3	Small scale DIY solar systems	28
2.2.4	Grid-connected system	29
2.2.5	Building systems	30
2.2.6	Power plants	31
2.2.7	Connection to a DC grid	31
2.2.8	Hybrid systems	32
2.2.9	Solar powered spacecraft	33
2.2.10	Solar propelled spacecraft	34
2.3	solar cell demand	35

CHAPTER 3: Material Properties and Solar Cell Efficiency

3.1	Properties of Material	36
3.1.1	Crystalline silicon	36
3.1.2	Thin films	38
3.1.2.1	Cadmium telluride solar cell	41
3.1.2.2	Copper indium gallium selenide	41
3.1.2.3	CIGS photovoltaic cells	42
3.1.2.4	General properties of high performance CIGS absorbers	43
3.1.2.5	Gallium arsenide multijunction	45
3.1.2.6	Light-absorbing dyes (DSSC)	46
3.1.2.7	Organic/polymer solar cells	47
3.1.2.8	Silicon thin films	48
3.2	Efficiency of solar cell	50
3.2.1	Energy conversion efficiency	50
3.2.2	Thermodynamic efficiency limit	51
3.2.3	Quantum efficiency	52
3.2.4	Maximum-power point	54
3.2.5	Fill factor	56
3.2.6	Comparison of energy conversion efficiencies	57
3.2.7	Solar cells and energy payback	59
3.3	System performance	60
3.3.1	Insolation and energy	60
3.3.2	Tracking the	60

3.3.3	Shading and dirt	61
3.3.4	Temperature	62
3.3.5	Module efficiency	63
3.3.6	Monitoring	63
3.3.7	Performance factors	63
3.3.8	Module life	64
3.3.9	Components	64
3.3.9.1	Trackers	64
3.3.9.2	Inverters	65

CHAPTER 4: MODELING OF THIN FILM SOLAR CELL

4.1	Modeling Parameters	67
4.1.1	CIGS Absorber	68
4.1.2	Transparent Front Contact	68
4.1.3	Transmission of Light	69
4.1.4	Back Contact	71
4.1.5	Bandgap and Carrier Lifetime	71
4.1.6	Cell width	72
4.1.7	Effect of carrier mobility on Efficiency-cell width relation	72
4.1.8	Temperature Effect	73

CHAPTER 5: SIMULATION, RESULTS AND DISCUSSION

5.1. Parameters Adjustment	74
5.2 Transmittance Optimization	74
5.3 Recombination Lifetime Optimization	77
5.4 Temperature Optimization	77
5.5 Cell Width Optimization	78
5.6 Fill Factor-Cell Width Relation	80

CHAPTER 6: CONCLUSION AND SUGGESTION

6.1 Conclusion	81
6.2 Suggestion for Future Works	81

REFERENCES	63
-------------------	-----------

LIST OF FIGURES

Fig: 1-1. Energy conversion by solar cell	01
Fig: 1-2. Microscopic view of solar cell	02
Fig:1-3 A solar cell made from a monocrystalline silicon wafer	03
Fig: 2-1. Photons in sunlight hit the solar panel and absorbed	08
Fig: 2-2. Band diagram of a silicon solar cell	10
Fig: 2-3. Operating principle of p-n junction	11
Fig: 2-4. p-n junction Photovoltaic cell	13
Fig: 2-5. The equivalent circuit of a solar cell	13
Fig: 2-6. The schematic symbol of a solar cell	14
Fig: 2-7. Equivalent circuit of one diode model	14
Fig: 2-8. Effect of temperature on the current-voltage characteristics of a solar cell	20
Fig: 2-9. Effect of series resistance on the current-voltage characteristics of a solar cell	21
Fig: 2-10. Effect of shunt resistance on the current–voltage characteristics of a solar cell	22
Fig: 2-11. Effect of reverse saturation current on the current-voltage characteristics of a solar cell	23
Fig: 2-12. Effect of ideality factor on the current-voltage characteristics of a solar cell	25
Fig: 2-13. Solar powered parking meter	26
Fig: 2-14. Schematic of a bare-bones off-grid system	27
Fig: 2-15. Off-grid PV system with battery charge	27
Fig: 2-16. Solar car	28

Fig: 2-17. Diagram of a residential grid-connected PV system	29
Fig: 2-18. Solar cell array on roof top	30
Fig: 2-19. Waldpolenz Solar Park, Germany	31
Fig: 2-20. Hybrid system	32
Fig: 2-21. PV on the International Space Station	33
Fig: 2-22. Solar Propelled Spacecraft	34
Fig: 2-23. Development of PV world market in MW _{peak} (MW _{peak} is defined as power under full sun, approx 1kW/m ²)	35
Fig: 3-1. Basic structure of a silicon based solar cell and its working mechanism.	38
Fig: 3-2. Cross-section of thin film polycrystalline solar cell	40
Fig: 3-3. Market share of the different PV technologies	41
Fig: 3-4. CIGS device structure	43
Fig: 3-5. CIGS unit cell. Red = Cu, Yellow = Se, Blue = In/Ga	44
Fig: 3-6. Efficiency vs Bandgap energy	52
Fig: 3-7. IQE, EQE, Reflectance vs Wavelength	55
Fig-3.8- I-V characteristics curve	57
Fig: 3-9. Comparison of energy conversion efficiencies	59
Fig: 3-10 Sun tracker	62
Fig: 3-11. Inverter for grid connected PV	67
Fig: 3-12. I-V characteristics curve	68
Fig: 4-1. Equivalent circuit of heterojunction solar cell	69
Fig: 4-2. Transmittance of ZnO:Al layer as a function of sheet resistance	71
Fig-5.1. Simulation showing module efficiency at different transmittance. Three different approximations describe the cell width of the solar cell.	76

Fig-5.2. Simulation showing module efficiency at different recombination life time. Three different bandgap energy influences on the shape of the curve.	77
Fig-5.3. Simulation showing module efficiency at different temperatures.	78
Fig-5.4. Simulation showing module efficiency at different base width. At different values of carrier mobility, the pattern of the curve has changed	79
Fig-5.5. Variation of fill factor (FF) with cell width of a given range (3mm-9mm)	80

CHAPTER 1

INTRODUCTION

1.1 General

A *solar cell* (also called *photovoltaic cell* or *photoelectric cell*) is a solid state electrical device that converts the energy of light directly into electricity by the *photovoltaic effect*. Incident photons are absorbed to photogenerate charge carriers that pass through an external load to do electrical work.



Fig: 1-1. Energy conversion by solar cell

Assemblies of solar cells are used to make solar modules which are used to capture energy from sunlight. When multiple modules are assembled together (such as prior to installation on a pole-mounted tracker system), the resulting integrated group of modules all oriented in one plane is referred to in the solar industry as a solar panel. The general public and some casual writers often refer to solar modules incorrectly as solar panels; technically this is not the correct usage of terminology. Nevertheless, both designations are seen in regular use, in reference to what are actually solar modules. The distinction between a module and a panel is that a module cannot be disassembled into smaller re-usable components in the field, whereas a solar panel is assembled from, and can be disassembled back into a stack of solar modules. The electrical energy generated from solar modules, referred to as solar power, is an example of solar energy.

Photovoltaics is the field of technology and research related to the practical application of photovoltaic cells in producing electricity from light, though it is often used specifically to refer to the generation of electricity from sunlight.

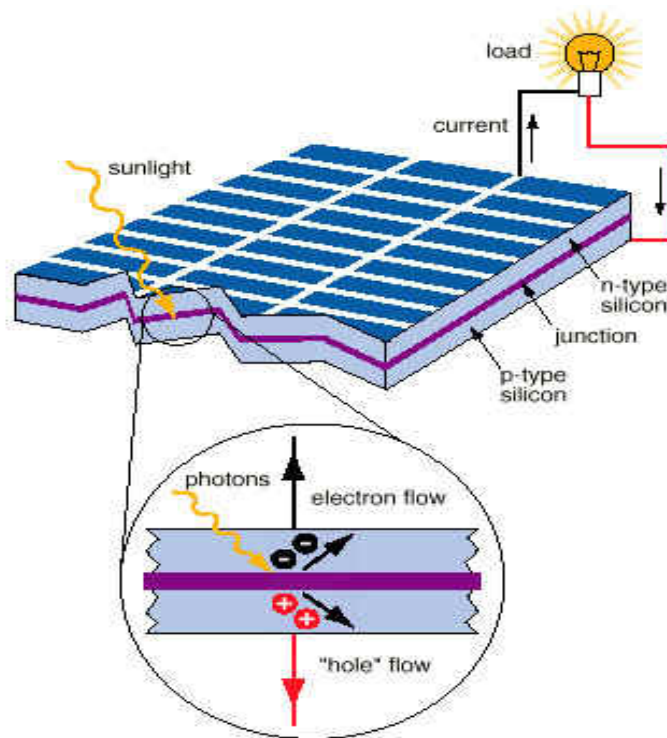


Fig: 1-2. Microscopic view of solar cell

Cells are described as *photovoltaic cells* when the light source is not necessarily sunlight. These are used for detecting light or other electromagnetic radiation near the visible range, for example infrared detectors, or measurement of light intensity.



Figure 1-3 A solar cell made from a monocrystalline silicon wafer

1.2 Solar Cell History

The term "photovoltaic" comes from the Greek $\phi\tilde{\omega}\varsigma$ (*phōs*) meaning "light", and "voltaic", from the name of the Italian physicist Volta, after whom a unit of electro-motive force, the volt, is named. The term "photo-voltaic" has been in use in English since 1849 [1].

The photovoltaic effect was first recognized in 1839 by French physicist A. E. Becquerel. However, it was not until 1883 that the first photovoltaic cell was built, by Charles Fritts, who coated the semiconductor selenium with an extremely thin layer of gold to form the junctions. The device was only around 1% efficient. In 1888 Russian physicist Aleksandr Stoletov built the first photoelectric cell based on the outer photoelectric effect discovered by Heinrich Hertz earlier in 1887.

Albert Einstein explained the photoelectric effect in 1905 for which he received the Nobel prize in Physics in 1921.^[2] Russell Ohl patented the modern junction semiconductor solar cell in 1946,^[3] which was discovered while working on the series of advances that would lead to the transistor.

1.2.1 First Practical Cell

The modern photovoltaic cell was developed in 1954 at Bell Laboratories.^[4] The highly efficient solar cell was first developed by Daryl Chapin, Calvin Souther Fuller and Gerald Pearson in 1954 using a diffused silicon p-n junction.^[5] At first, cells were developed for toys and other minor uses, as the cost of the electricity they produced was very high; in relative terms, a cell that produced 1 watt of electrical power in bright sunlight cost about \$250, comparing to \$2 to \$3 for a coal plant.

Solar cells were rescued from obscurity by the suggestion to add them to the Vanguard I satellite, launched in 1958. In the original plans, the satellite would be powered only by battery, and last a short time while this ran down. By adding cells to the outside of the body, the mission time could be extended with no major changes to the spacecraft or its power systems. There was some scepticism at first, but in practice the cells proved to be a huge success, and solar cells were quickly designed into many new satellites, notably Bell's own Telstar.

Improvements were slow over the next two decades, and the only widespread use was in space applications where their power-to-weight ratio was higher than any competing technology. However, this success was also the reason for slow progress; space users were willing to pay anything for the best possible cells, there was no reason to invest in lower-cost solutions if this would reduce efficiency. Instead, the price of cells was determined largely by the semiconductor industry; their move to integrated circuits in the 1960s led to the availability of larger boules at lower relative prices. As their price fell, the price of the resulting cells did as well. However these effects were limited, and by 1971 cell costs were estimated to be \$100 per watt.

1.2.2 Berman's Price Reductions

In the late 1960s, Elliot Berman was investigating a new method for producing the silicon feedstock in a ribbon process. However, he found little interest in the project and was unable

to gain the funding needed to develop it. In a chance encounter, he was later introduced to a team at Exxon who were looking for projects 30 years in the future. The group had concluded that electrical power would be much more expensive by 2000, and felt that this increase in price would make new alternative energy sources more attractive, and solar was the most interesting among these. In 1969, Berman joined the Linden, New Jersey Exxon lab, Solar Power Corporation (SPC).^[6]

His first major effort was to canvas the potential market to see what possible uses for a new product were, and they quickly found that if the price per watt were reduced from then-current \$100/watt to about \$20/watt there would be significant demand. Knowing that his ribbon concept would take years to develop, the team started looking for ways to hit the \$20 price point using existing materials.^[6]

The first improvement was the realization that the existing cells were based on standard semiconductor manufacturing process, even though that was not ideal. This started with the boule, cutting it into disks called wafers, polishing the wafers, and then, for cell use, coating them with an anti-reflective layer. Berman noted that the rough-sawn wafers already had a perfectly suitable anti-reflective front surface, and by printing the electrodes directly on this surface, two major steps in the cell processing were eliminated. The team also explored ways to improve the mounting of the cells into arrays, eliminating the expensive materials and hand wiring used in space applications. Their solution was to use a printed circuit board on the back, acrylic plastic on the front, and silicone glue between the two, potting the cells. The largest improvement in price point was Berman's realization that existing silicon was effectively "too good" for solar cell use; the minor imperfections that would ruin a boule (or individual wafer) for electronics would have little effect in the solar application.^[7] Solar cells could be made using cast-off material from the electronics market.

Putting all of these changes into practice, the company started buying up "reject" silicon from existing manufacturers at very low cost. By using the largest wafers available, thereby reducing the amount of wiring for a given panel area, and packaging them into panels using their new methods, by 1973 SPC was producing panels at \$10 per watt and selling them at \$20 per watt, a fivefold decrease in prices in two years

1.2.3 Further Improvements

In the time since Berman's work, improvements have brought production costs down under \$1 a watt, with wholesale costs well under \$2. "Balance of system" costs are now more than the panels themselves. Large commercial arrays can be built at below \$3.40 a watt,^{[8][9]} fully commissioned.

As the semiconductor industry moved to ever-larger boules, older equipment became available at fire-sale prices. Cells have grown in size as older equipment became available on the surplus market; ARCO Solar's original panels used cells with 2 to 4 inch (51 to 100 mm) diameter. Panels in the 1990s and early 2000s generally used 5 inch (125 mm) wafers, and since 2008 almost all new panels use 6 inch (150 mm) cells. Another major change was the move to polycrystalline silicon. This material has less efficiency, but is less expensive to produce in bulk. The widespread introduction of flat screen televisions in the late 1990s and early 2000s led to the wide availability of large sheets of high-quality glass, used on the front of the panels.

1.3 Objective

Based on the background summarized in the foregoing sections, the present research aims at covering the following objectives to improve the efficiency of thin film solar cell. The objectives are-

- ❖ To find the optimal point of different parameters.
- ❖ To determine the value of intermediate bandgap energy for heterojunction solar cell.
- ❖ To find out the optimum temperature and carrier recombination life time.
- ❖ To find out the transmittance value.

1.4 Structure of the Thesis

The thesis consists of six chapters in which the current one is Chapter 1. This chapter gives the general background of solar cell and the objectives of this thesis work. The first half of chapter 2 gives a detail picture on the working phenomenon of a solar cell in general. It also discuss about the behavior of solar cell on different criteria. In the second half of this chapter we have tried to highlight various application of solar cell and also the increasing demand of it. In Chapter 3 we have discussed about the properties of thin film solar cell materials with respect to other solar cell materials. The later part of this chapter gives an overview on solar cell efficiency and system performance.

In Chapter 4, the modeling of a solar cell is discussed where we have provided the different the relationships between the parameters. Simulation and results are presented in chapter-5. This is a vital chapter in which all of the simulated curves hold the optimal points of different parameters that can make a better efficiency of solar cell. At last, Chapter-6 bears the conclusion part of our thesis.

CHAPTER 2

THEORY AND APPLICATION OF SOLAR CELL

2.1 Theory of Solar Cell

The **theory of solar cells** explains the physical processes by which light is converted into electrical current when striking a suitable semiconductor device. The theoretical studies are of practical use because they predict the fundamental limits of solar cell performance, and give guidance on the phenomena that contribute to losses and solar cell efficiency.

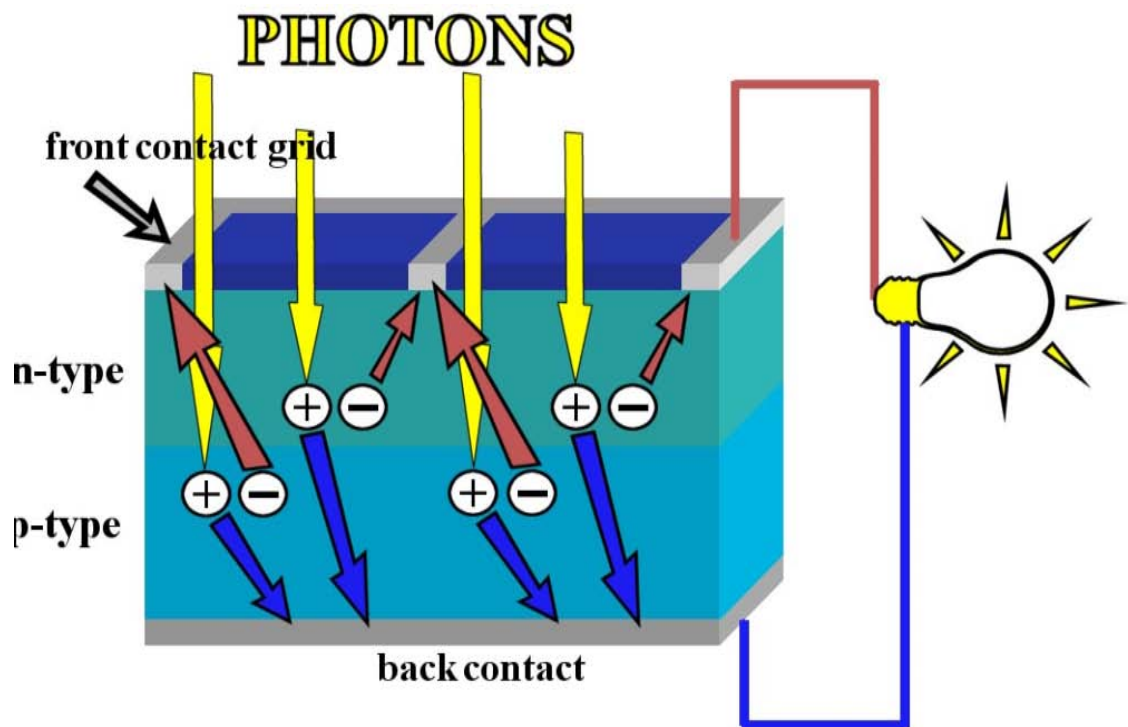


Fig: 2-1. Photons in sunlight hit the solar panel and absorbed

2.1.1 Simple Explanation

1. Photons in sunlight hit the solar panel and are absorbed by semiconducting materials, such as silicon.
2. Electrons (negatively charged) are knocked loose from their atoms, allowing them to flow through the material to produce electricity. Due to the special composition of solar cells, the electrons are only allowed to move in a single direction.
3. An array of solar cells converts solar energy into a usable amount of direct current (DC) electricity.

2.1.2 Photogeneration of Charge Carriers

When a photon hits a piece of silicon, one of three things can happen:

1. The photon can pass straight through the silicon — this (generally) happens for lower energy photons,
2. The photon can reflect off the surface,
3. The photon can be absorbed by the silicon, if the photon energy is higher than the silicon band gap value. This generates an electron-hole pair and sometimes heat, depending on the band structure.

When a photon is absorbed, its energy is given to an electron in the crystal lattice. Usually this electron is in the valence band, and is tightly bound in covalent bonds between neighboring atoms, and hence unable to move far. The energy given to it by the photon "excites" it into the conduction band, where it is free to move around within the semiconductor. The covalent bond that the electron was previously a part of now has one fewer electron — this is known as a hole. The presence of a missing covalent bond allows the bonded electrons of neighboring atoms to move into the "hole," leaving another hole behind, and in this way a hole can move through the lattice. Thus, it can be said that photons absorbed in the semiconductor create mobile electron-hole pairs.

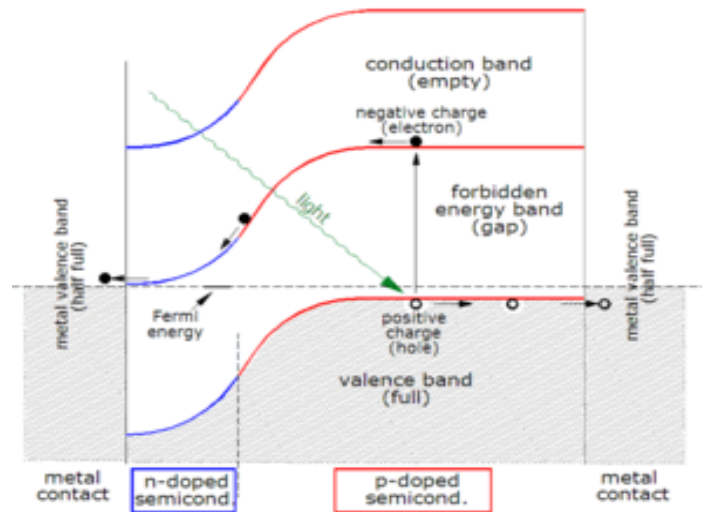


Fig: 2-2. Band diagram of a silicon solar cell

A photon need only have greater energy than that of the band gap in order to excite an electron from the valence band into the conduction band. However, the solar frequency spectrum approximates a black body spectrum at about 5,800 K,^[10] and as such, much of the solar radiation reaching the Earth is composed of photons with energies greater than the band gap of silicon. These higher energy photons will be absorbed by the solar cell, but the difference in energy between these photons and the silicon band gap is converted into heat (via lattice vibrations — called phonons) rather than into usable electrical energy.

2.1.3 Charge Carrier Separation

There are two main modes for charge carrier separation in a solar cell:

1. **Drift** of carriers, driven by an electric field established across the device
2. **Diffusion** of carriers due to their random thermal motion, until they are captured by the electrical fields existing at the edges of the active region.

In thick solar cells there is no electric field in the active region, so the dominant mode of charge carrier separation is diffusion. In these cells the diffusion length of minority carriers (the length that photo-generated carriers can travel before they recombine) must be large compared to the cell thickness. In thin film cells (such as amorphous silicon), the diffusion length of minority carriers is usually very short due to the existence of defects, and the dominant charge separation is therefore drift, driven by the electrostatic field of the junction, which extends to the whole thickness of the cell^[2].

2.1.4 The *p-n* Junction

The most commonly known solar cell is configured as a large-area *p-n* junction made from silicon. As a simplification, one can imagine bringing a layer of *n*-type silicon into direct contact with a layer of *p*-type silicon. In practice, *p-n* junctions of silicon solar cells are not made in this way, but rather by diffusing an *n*-type dopant into one side of a *p*-type wafer (or vice versa).

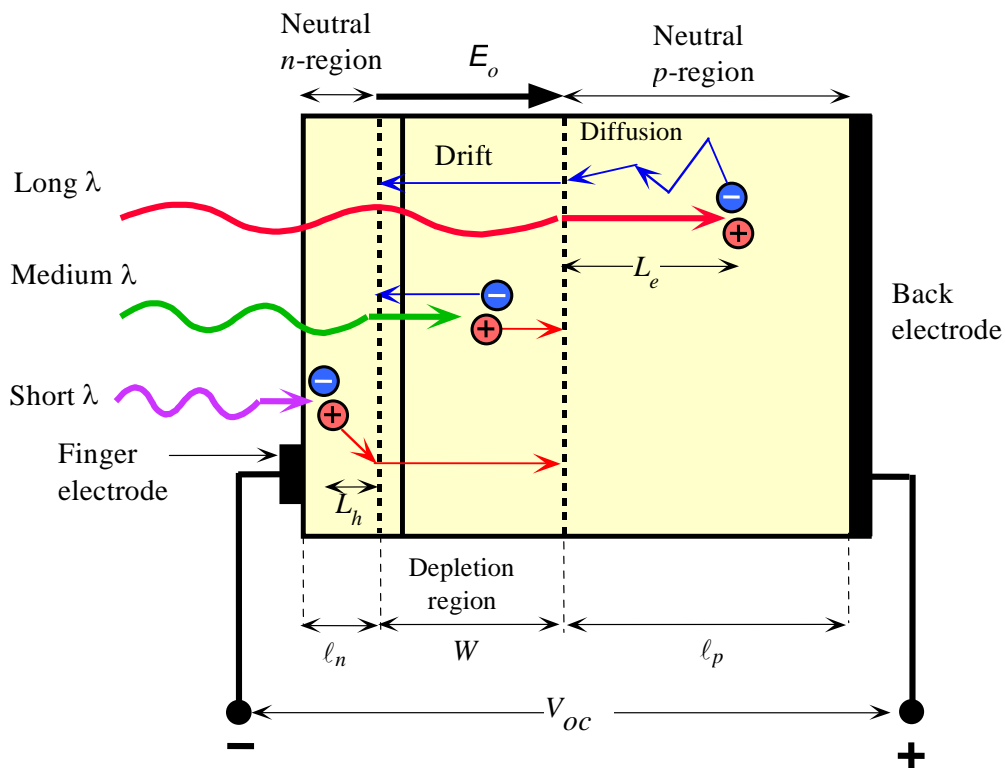


Fig: 2-3. Operating principle of *p-n* junction

If a piece of p-type silicon is placed in intimate contact with a piece of n-type silicon, then a diffusion of electrons occurs from the region of high electron concentration (the n-type side of the junction) into the region of low electron concentration (p-type side of the junction). When the electrons diffuse across the p-n junction, they recombine with holes on the p-type side. The diffusion of carriers does not happen indefinitely, however, because charges build up on either side of the junction and create an electric field. The electric field creates a diode that promotes charge flow, known as drift current that opposes and eventually balances out the diffusion of electrons and holes. This region where electrons and holes have diffused across the junction is called the depletion region because it no longer contains any mobile charge carriers. It is also known as the *space charge region*.

Ohmic metal-semiconductor contacts are made to both the n-type and p-type sides of the solar cell, and the electrodes connected to an external load. Electrons that are created on the n-type side, or have been "collected" by the junction and swept onto the n-type side, may travel through the wire, power the load, and continue through the wire until they reach the p-type semiconductor-metal contact. Here, they recombine with a hole that was either created as an electron-hole pair on the p-type side of the solar cell, or a hole that was swept across the junction from the n-type side after being created there.

The voltage measured is equal to the difference in the quasi Fermi levels of the minority carriers, i.e. electrons in the p-type portion and holes in the n-type portion.

2.1.5 Equivalent Circuit of a Solar Cell

To understand the electronic behavior of a solar cell, it is useful to create a model which is electrically equivalent, and is based on discrete electrical components whose behavior is well known. An ideal solar cell may be modeled by a current source in parallel with a diode; in practice no solar cell is ideal, so a shunt resistance and a series resistance component are added to the model.

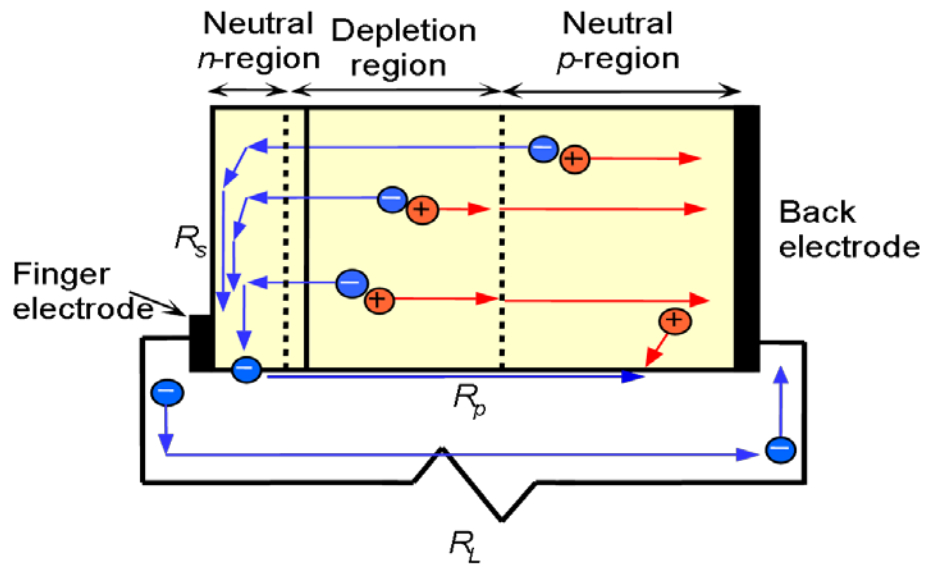


Fig: 2-4. *p-n* junction Photovoltaic cell

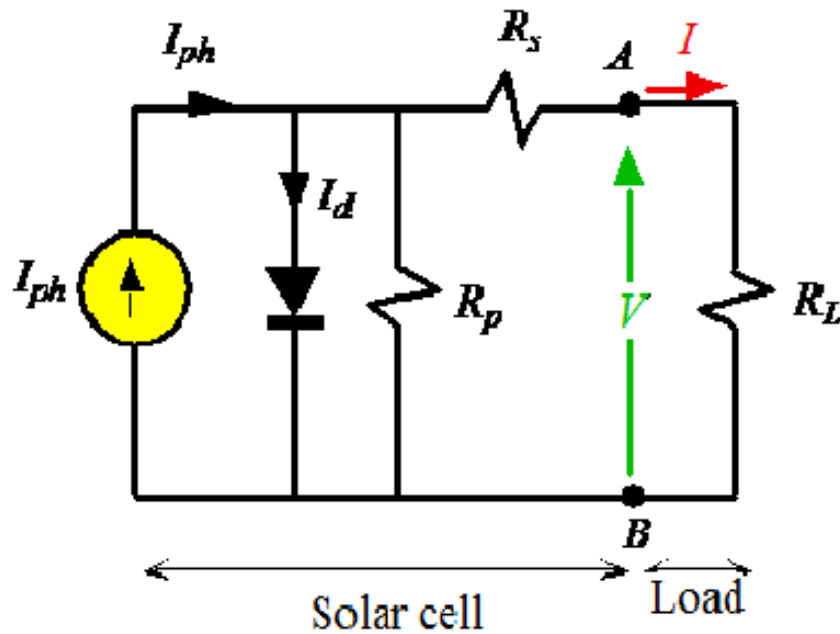


Fig: 2-5. The equivalent circuit of a solar cell

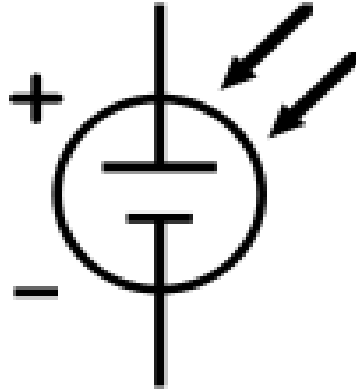


Fig: 2-6. The schematic symbol of a solar cell

The resulting equivalent circuit of a solar cell is shown on the above and also the schematic representation of a solar cell for use in circuit diagrams.

2.1.6 One-Diode Model

A solar cell can be modeled as an electric circuit in the so-called one-diode model. The one-diode model consists of a current generator in parallel with a diode and a shunt resistance, R_{sh} , which are all connected in series with a series resistance, R_s . The equivalent circuit is shown below. An equation for the one-diode model is derived using the equivalent circuit and the diode equation

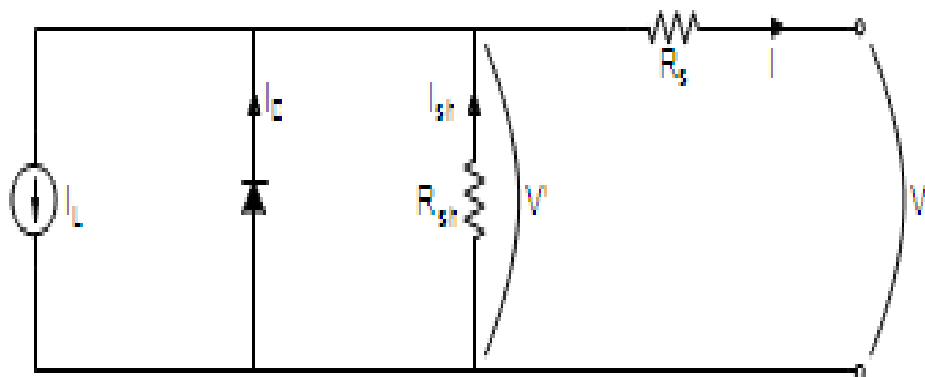


Fig: 2-7. Equivalent circuit of one diode model

Following Kirchhoff's current law

$$I = I_D + I_{sh} - I_L \text{ ----- (1)}$$

Kirchhoff's voltage law and Ohm's law give

$$V_0 = V - IR_s \text{ ----- (2)}$$

The diode equation and Eq. 2 give

$$I_D = I_0(e^{qV_0/AkT} - 1) = I_0(e^{q(V - IR_s)/AkT} - 1) \text{ ----- (3)}$$

Ohm's law and Eq. 2 gives

$$I_{sh} = V_0/R_{sh} = (V - IR_s)/R_{sh} \text{ ----- (4)}$$

Finally, Eq. 3 and Eq. 4 in Eq. 1 give an equation for the one-diode model

$$I = I_0(e^{q(V - IR_s)/AkT} - 1) + (V - IR_s)/R_{sh} - I_L \text{ ----- (5)}$$

2.1.7 Characteristic Equation

From the equivalent circuit it is evident that the current produced by the solar cell is equal to that produced by the current source, minus that which flows through the diode, minus that which flows through the shunt resistor:^[11]

$$I = I_L - I_D - I_{SH}$$

where

- I = output current (amperes)
- I_L = photogenerated current (amperes)

- I_D = diode current (amperes)
- I_{SH} = shunt current (amperes).

The current through these elements is governed by the voltage across them:

$$V_j = V + IR_S$$

where

- V_j = voltage across both diode and resistor R_{SH} (volts)
- V = voltage across the output terminals (volts)
- I = output current (amperes)
- R_S = series resistance (Ω).

By the Shockley diode equation, the current diverted through the diode is:

$$I_D = I_0 \left\{ \exp \left[\frac{qV_j}{nkT} \right] - 1 \right\}$$

where

- I_0 = reverse saturation current (amperes)
- n = diode ideality factor (1 for an ideal diode)
- q = elementary charge
- k = Boltzmann's constant
- T = absolute temperature
- At 25°C, $kT/q \approx 0.0259$ volts.

By Ohm's law, the current diverted through the shunt resistor is:

$$I_{SH} = \frac{V_j}{R_{SH}}$$

where

R_{SH} = shunt resistance (Ω).

Substituting these into the first equation produces the characteristic equation of a solar cell, which relates solar cell parameters to the output current and voltage:

$$I = I_L - I_0 \left\{ \exp \left[\frac{q(V + IR_S)}{nkT} \right] - 1 \right\} - \frac{V + IR_S}{R_{SH}}.$$

An alternative derivation produces an equation similar in appearance, but with V on the left-hand side. The two alternatives are identities; that is, they yield precisely the same results.

In principle, given a particular operating voltage V the equation may be solved to determine the operating current I at that voltage. However, because the equation involves I on both sides in a transcendental function the equation has no general analytical solution. However, even without a solution it is physically instructive. Furthermore, it is easily solved using numerical methods. (A general analytical solution to the equation is possible using Lambert's W function, but since Lambert's W generally itself must be solved numerically this is a technicality.)

Since the parameters I_0 , n , R_S , and R_{SH} cannot be measured directly, the most common application of the characteristic equation is nonlinear regression to extract the values of these parameters on the basis of their combined effect on solar cell behavior.

2.1.8 Open-Circuit Voltage and Short-Circuit Current

When the cell is operated at open circuit, $I = 0$ and the voltage across the output terminals is defined as the *open-circuit voltage*. Assuming the shunt resistance is high enough to neglect the final term of the characteristic equation, the open-circuit voltage V_{OC} is:

$$V_{OC} \approx \frac{kT}{q} \ln \left(\frac{I_L}{I_0} + 1 \right).$$

Similarly, when the cell is operated at short circuit, $V = 0$ and the current I through the terminals is defined as the *short-circuit current*. It can be shown that for a high-quality solar cell (low R_S and I_0 , and high R_{SH}) the short-circuit current I_{SC} is:

$$I_{SC} \approx I_L.$$

It should be noted that it is not possible to extract any power from the device when operating at either open circuit or short circuit conditions.

2.1.9 Effect of Physical Size

The values of I_0 , R_S , and R_{SH} are dependent upon the physical size of the solar cell. In comparing otherwise identical cells, a cell with twice the surface area of another will, in principle, have double the I_0 because it has twice the junction area across which current can leak. It will also have half the R_S and R_{SH} because it has twice the cross-sectional area through which current can flow. For this reason, the characteristic equation is frequently written in terms of current density, or current produced per unit cell area:

$$J = J_L - J_0 \left\{ \exp \left[\frac{q(V + Jr_S)}{nkT} \right] - 1 \right\} - \frac{V + Jr_S}{r_{SH}}$$

where

- J = current density (amperes/cm²)
- J_L = photogenerated current density (amperes/cm²)
- J_0 = reverse saturation current density (amperes/cm²)
- r_S = specific series resistance (Ω -cm²)
- r_{SH} = specific shunt resistance (Ω -cm²).

This formulation has several advantages. One is that since cell characteristics are referenced to a common cross-sectional area they may be compared for cells of different physical dimensions. While this is of limited benefit in a manufacturing setting, where all cells tend to be the same size, it is useful in research and in comparing cells between manufacturers.

Another advantage is that the density equation naturally scales the parameter values to similar orders of magnitude, which can make numerical extraction of them simpler and more accurate even with naive solution methods.

There are practical limitations of this formulation. For instance, certain parasitic effects grow in importance as cell sizes shrink and can affect the extracted parameter values. Recombination and contamination of the junction tend to be greatest at the perimeter of the cell, so very small cells may exhibit higher values of J_0 or lower values of R_{SH} than larger cells that are otherwise identical. In such cases, comparisons between cells must be made cautiously and with these effects in mind.

This approach should only be used for comparing solar cells with comparable layout. For instance, a comparison between primarily quadratical solar cells like typical crystalline silicon solar cells and narrow but long solar cells like typical thin film solar cells can lead to wrong assumptions caused by the different kinds of current paths and therefore the influence of for instance a distributed series resistance r_s .

2.1.10 Cell Temperature

Temperature affects the characteristic equation in two ways: directly, via T in the exponential term, and indirectly via its effect on I_0 (strictly speaking, temperature affects all of the terms, but these two far more significantly than the others). While increasing T reduces the magnitude of the exponent in the characteristic equation, the value of I_0 increases exponentially with T . The net effect is to reduce V_{OC} (the open-circuit voltage) linearly with increasing temperature. The magnitude of this reduction is inversely proportional to V_{OC} ; that is, cells with higher values of V_{OC} suffer smaller reductions in voltage with increasing temperature. For most crystalline silicon solar cells the change in V_{OC} with temperature is about $-0.50\%/^{\circ}\text{C}$, though the rate for the highest-efficiency crystalline silicon cells is around $-0.35\%/^{\circ}\text{C}$. By way of comparison, the rate for amorphous silicon solar cells is $-0.20\%/^{\circ}\text{C}$ to $-0.30\%/^{\circ}\text{C}$, depending on how the cell is made.

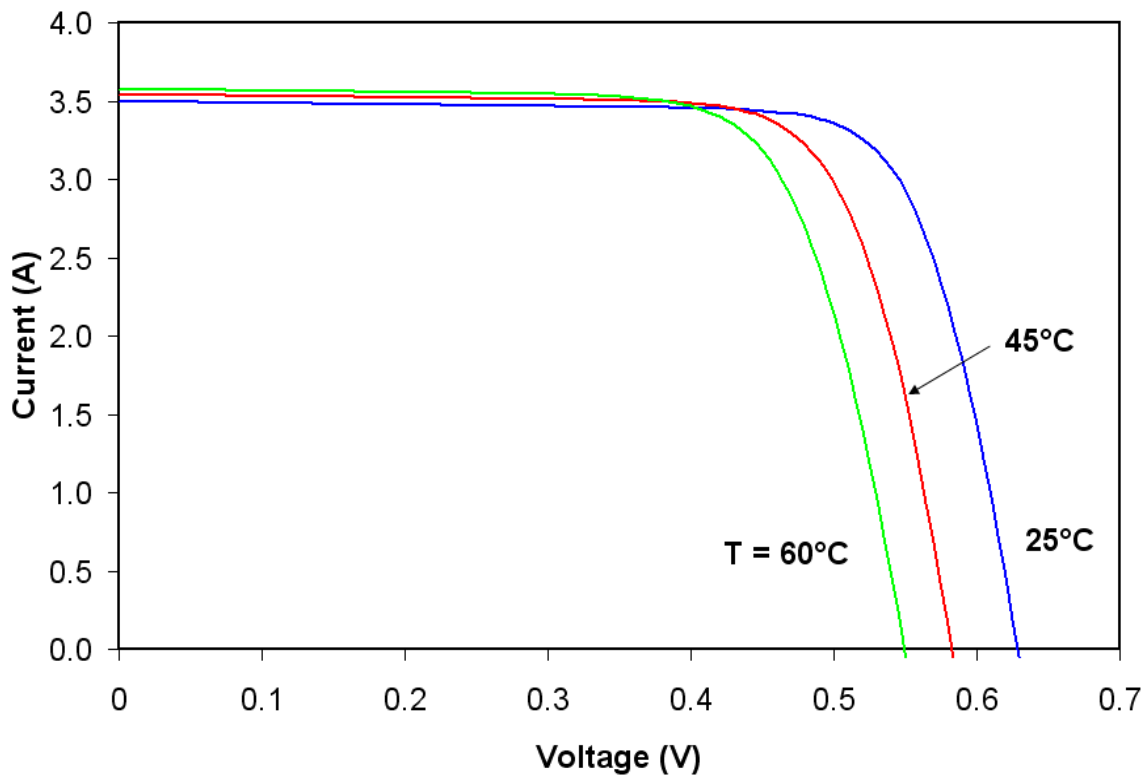


Fig: 2-8. Effect of temperature on the current-voltage characteristics of a solar cell

The amount of photogenerated current I_L increases slightly with increasing temperature because of an increase in the number of thermally generated carriers in the cell. This effect is slight, however: about 0.065%/°C for crystalline silicon cells and 0.09% for amorphous silicon cells.

The overall effect of temperature on cell efficiency can be computed using these factors in combination with the characteristic equation. However, since the change in voltage is much stronger than the change in current, the overall effect on efficiency tends to be similar to that on voltage. Most crystalline silicon solar cells decline in efficiency by 0.50%/°C and most amorphous cells decline by 0.15-0.25%/°C. The figure above shows I-V curves that might typically be seen for a crystalline silicon solar cell at various temperatures.

2.1.11 Resistance

It has both series and shunt resistance which is described below

2.1.11.1 Series Resistance

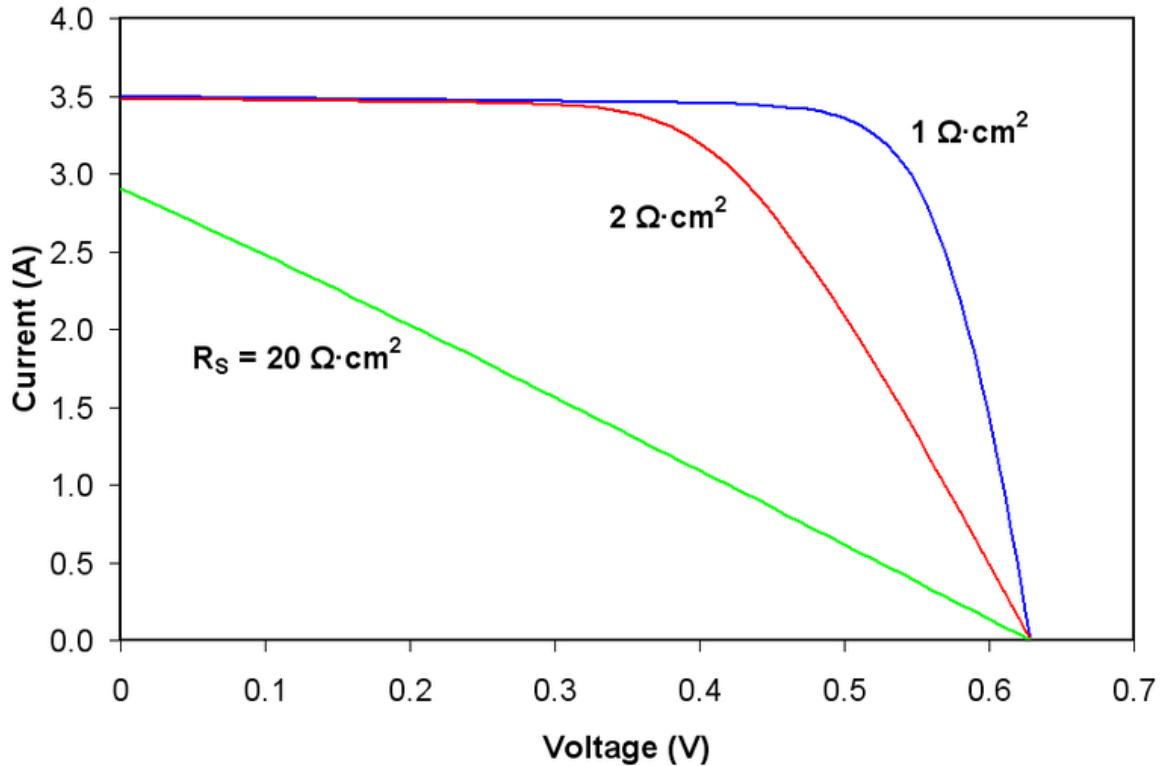


Fig: 2-9. Effect of series resistance on the current-voltage characteristics of a solar cell

As series resistance increases, the voltage drop between the junction voltage and the terminal voltage becomes greater for the same current. The result is that the current-controlled portion of the I-V curve begins to sag toward the origin, producing a significant decrease in the terminal voltage V and a slight reduction in I_{SC} , the short-circuit current. Very high values of R_s will also produce a significant reduction in I_{SC} ; in these regimes, series resistance dominates and the behavior of the solar cell resembles that of a resistor. These effects are shown for crystalline silicon solar cells in the I-V curves displayed in the figure to the right.

Losses caused by series resistance are in a first approximation given by $P_{\text{loss}} = V_{R_S} I = I^2 R_S$ and increase quadratically with (photo-) current. Series resistance losses are therefore most important at high illumination intensities.

2.1.11.2 Shunt Resistance

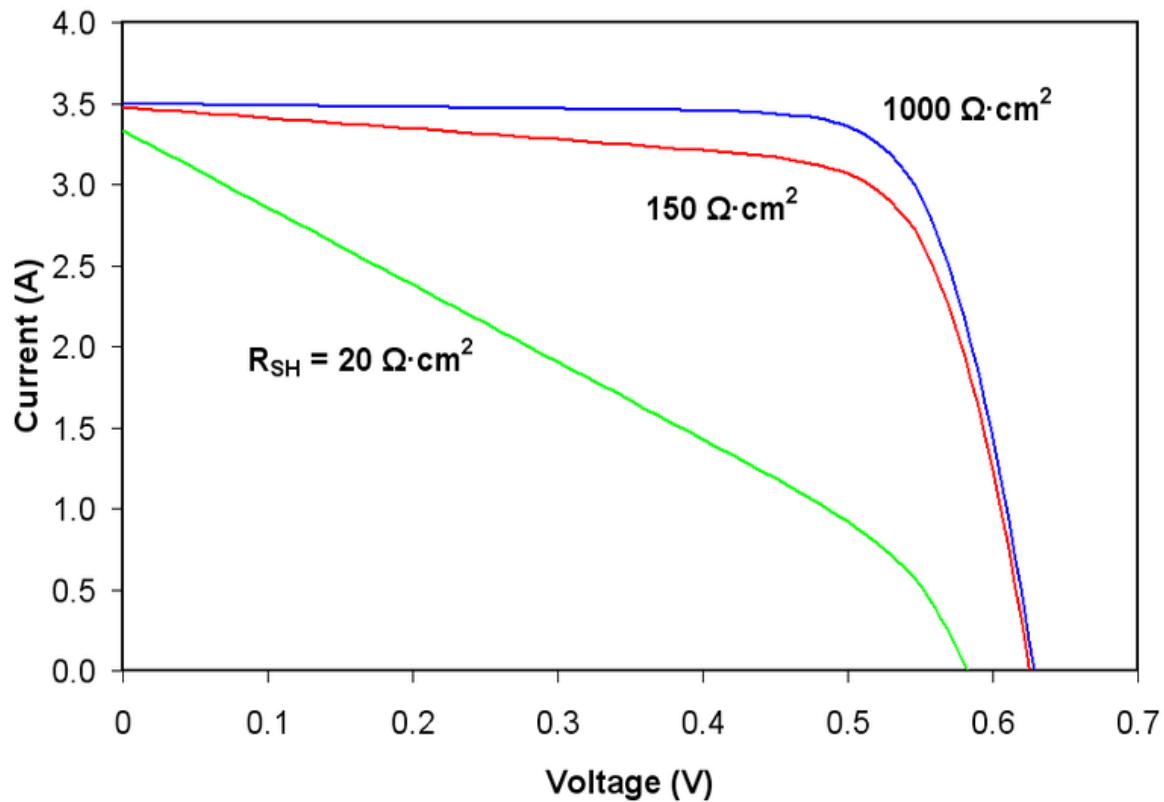


Fig: 2-10. Effect of shunt resistance on the current–voltage characteristics of a solar cell

As shunt resistance decreases, the current diverted through the shunt resistor increases for a given level of junction voltage. The result is that the voltage-controlled portion of the I-V curve begins to sag toward the origin, producing a significant decrease in the terminal current I and a slight reduction in V_{OC} . Very low values of R_{SH} will produce a significant reduction in V_{OC} . Much as in the case of a high series resistance, a badly shunted solar cell will take on operating characteristics similar to those of a resistor. These effects are shown for crystalline silicon solar cells in the I-V curves displayed in the figure to the right.

2.1.12 Reverse Saturation Current

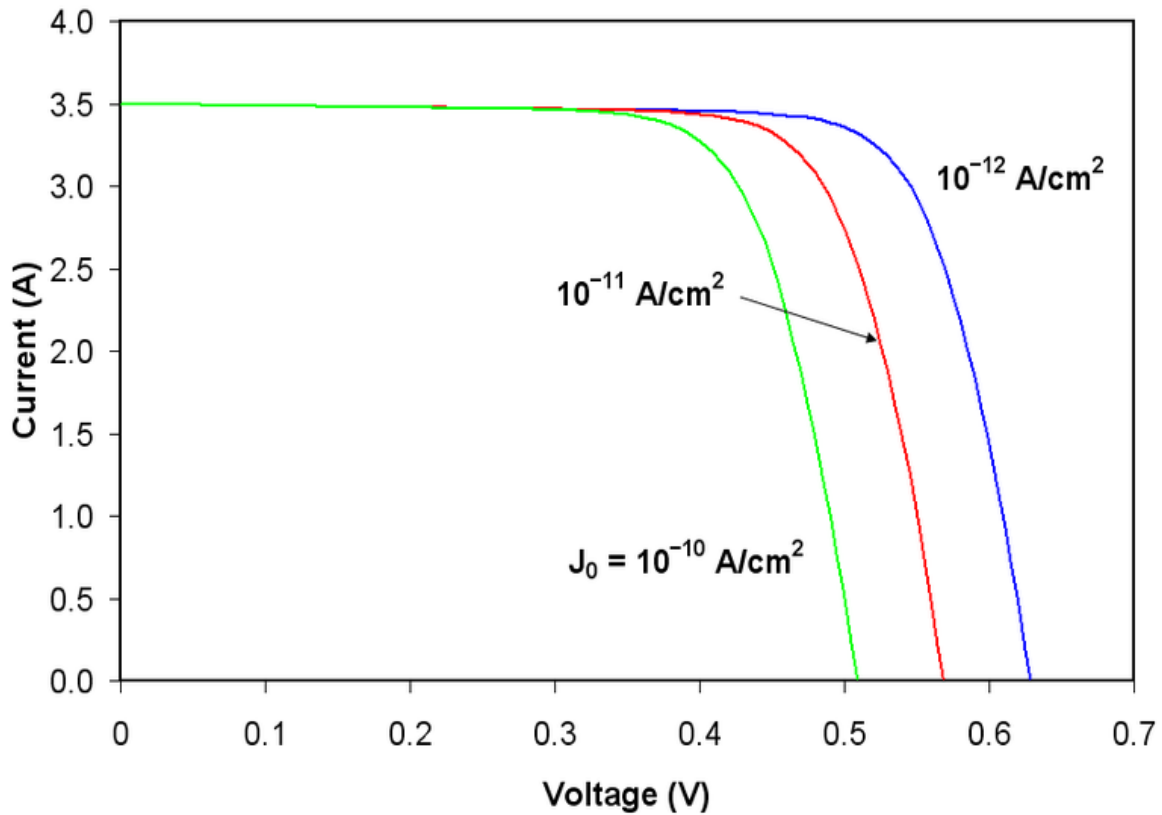


Fig: 2-11. Effect of reverse saturation current on the current-voltage characteristics of a solar cell

If one assumes infinite shunt resistance, the characteristic equation can be solved for V_{OC} :

$$V_{OC} = \frac{kT}{q} \ln \left(\frac{I_{SC}}{I_0} + 1 \right).$$

Thus, an increase in I_0 produces a reduction in V_{OC} proportional to the inverse of the logarithm of the increase. This explains mathematically the reason for the reduction in V_{OC} that accompanies increases in temperature described above. The effect of reverse saturation current on the I-V curve of a crystalline silicon solar cell are shown in the figure to the right. Physically, reverse saturation current is a measure of the "leakage" of carriers across the p-n

junction in reverse bias. This leakage is a result of carrier recombination in the neutral regions on either side of the junction.

2.1.13 Transmittance

The transmittance is the fraction of incident light at a specified wavelength that passes through a sample

$$T(\lambda) = I_{out} / I_{in}$$

where I_{in} is the intensity of the incident light and I_{out} is the intensity of the light coming out of the sample. The transmittance can also be expressed using the exponential Beer-Lambert law

$$T(\lambda) = e^{-\alpha(\lambda)d}$$

Where $\alpha(\lambda)$ is the attenuation coefficient and d is the path length.

2.1.14 Ideality Factor

The ideality factor (also called the emissivity factor) is a fitting parameter that describes how closely the diode's behavior matches that predicted by theory, which assumes the p-n junction of the diode is an infinite plane and no recombination occurs within the space-charge region. A perfect match to theory is indicated when $n = 1$. When recombination in the space-charge region dominates other recombination, however, $n = 2$. The effect of changing ideality factor independently of all other parameters is shown for a crystalline silicon solar cell in the I-V curves displayed in the figure to the right.

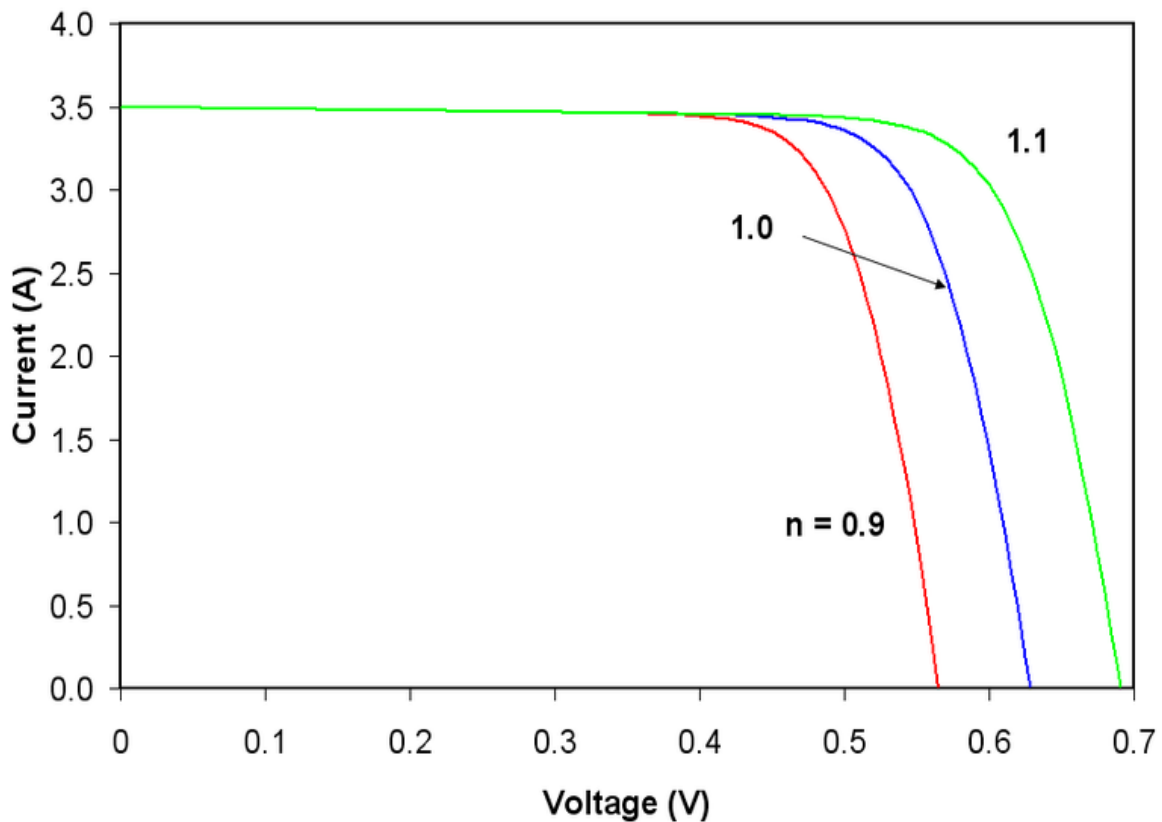


Fig: 2-12. Effect of ideality factor on the current-voltage characteristics of a solar cell

Most solar cells, which are quite large compared to conventional diodes, well approximate an infinite plane and will usually exhibit near-ideal behavior under Standard Test Condition ($n \approx 1$). Under certain operating conditions, however, device operation may be dominated by recombination in the space-charge region. This is characterized by a significant increase in I_0 as well as an increase in ideality factor to $n \approx 2$. The latter tends to increase solar cell output voltage while the former acts to erode it. The net effect, therefore, is a combination of the increase in voltage shown for increasing n in the figure to the right and the decrease in voltage shown for increasing I_0 in the figure above. Typically, I_0 is the more significant factor and the result is a reduction in voltage.

2.2 Applications

Initially appearing as small strips powering hand-held calculators, thin-film PV is now available in very large modules used in sophisticated building-integrated installations and vehicle charging systems.

2.2.1 Standalone Systems



Fig: 2-13. Solar powered parking meter.

A standalone system does not have a connection to the electricity "mains" (aka "grid"). Standalone systems vary widely in size and application from wristwatches or calculators to remote buildings or spacecraft. If the load is to be supplied independently of solar insolation, the generated power is stored and buffered with a battery. In non-portable applications where weight is not an issue, such as in buildings, lead acid batteries are most commonly used for their low cost. A charge controller may be incorporated in the system to: a) avoid battery damage by excessive charging or discharging and, b) optimizing the production of the cells or modules by maximum power point tracking (MPPT). However, in simple PV systems where

the PV module voltage is matched to the battery voltage, the use of MPPT electronics is generally considered unnecessary, since the battery voltage is stable enough to provide near-maximum power collection from the PV module. In small devices (e.g. calculators, parking meters) only direct current (DC) is consumed. In larger systems (e.g. buildings, remote water pumps) AC is usually required. To convert the DC from the modules or batteries into AC, an inverter is used.

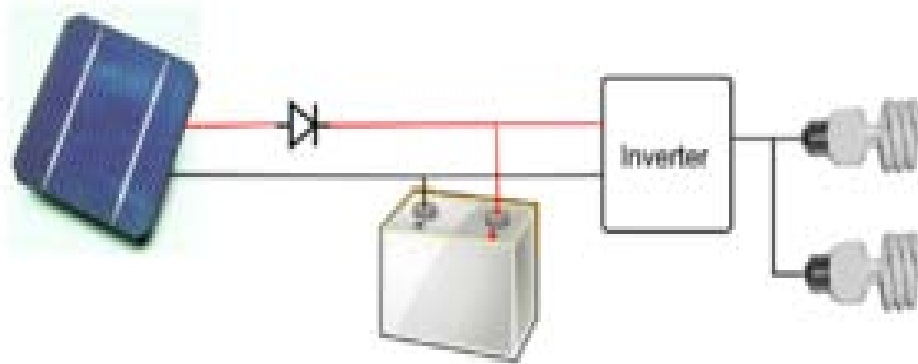


Fig: 2-14. Schematic of a bare-bones off-grid system

A schematic of a bare-bones off-grid system, consisting (from left to right) of photovoltaic module, a blocking-diode to prevent battery drain during low-insolation, a battery, an inverter, and an AC load such as a fluorescent lamp

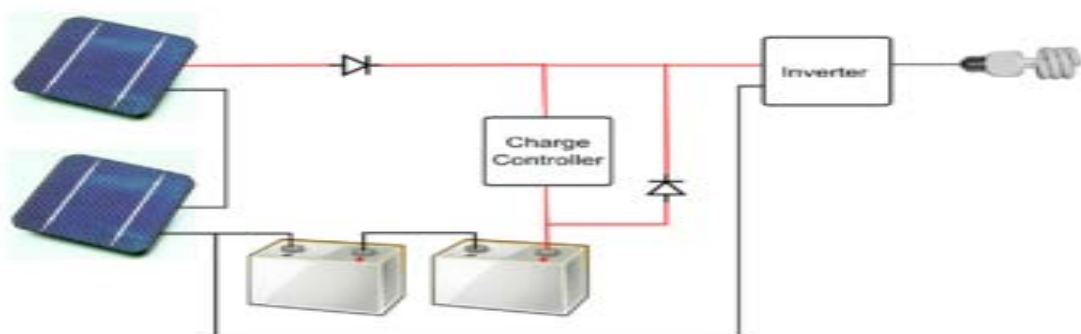


Fig: 2-15. Off-grid PV system with battery charge

2.2.2 Solar Vehicles

Ground, water, air or space vehicles may obtain some or all of the energy required for their operation from the sun. Surface vehicles generally require higher power levels than can be sustained by a practically-sized solar array, so a battery is used to meet peak power demand, and the solar array recharges it. Space vehicles have successfully used solar photovoltaic systems for years of operation, eliminating the weight of fuel or primary batteries.



Fig: 2-16. Solar car

2.2.3 Small scale DIY Solar SystemsWith a growing DIY-community and an increasing interest in environmentally friendly "green energy", some hobbyists have endeavored to build their own PV solar systems from kits ^[12] or partly diy.^[13] Usually, the DIY-community uses inexpensive ^[14] and/or high efficiency systems^[15](such as those with

solar tracking) to generate their own power. As a result, the DIY-systems often end up cheaper than their commercial counterparts.^[7] Often, the system is also hooked up into the regular power grid to repay part of the investment via net metering. These systems usually generate power amount of ~2 kW or less. Through the internet, the community is now able to obtain plans to construct the system (at least partly DIY) and there is a growing trend toward building them for domestic requirements. The DIY-PV solar systems are now also being used both in developed countries and in developing countries, to power residences and small businesses.

2.2.4 Grid-Connected System

A grid connected system is connected to a large independent grid (typically the public electricity grid) and feeds power into the grid. Grid connected systems vary in size from residential (2-10kWp) to solar power stations (up to 10s of GWp). This is a form of decentralized electricity generation. In the case of residential or building mounted grid connected PV systems, the electricity demand of the building is met by the PV system. Only the excess is fed into the grid when there is an excess. The feeding of electricity into the grid requires the transformation of DC into AC by a special, grid-controlled solar inverter.

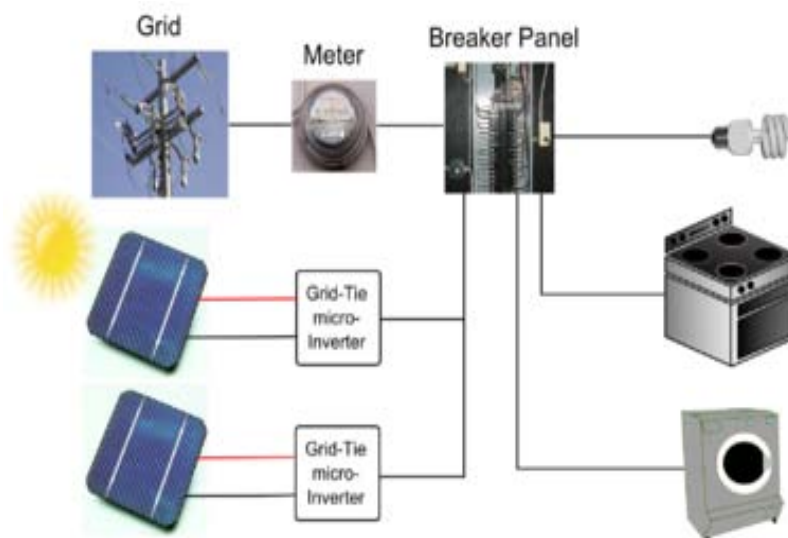


Fig: 2-17. Diagram of a residential grid-connected PV system

In kW sized installations the DC side system voltage is as high as permitted (typically 1000V except US residential 600V) to limit ohmic losses. Most modules (72 crystalline silicon cells) generate about 160W at 36 volts. It is sometimes necessary or desirable to connect the modules partially in parallel rather than all in series. One set of modules connected in series is known as a 'string'.

2.2.5 Building Systems

In urban and suburban areas, photovoltaic arrays are commonly used on rooftops to supplement power use; often the building will have a connection to the power grid, in which case the energy produced by the PV array can be sold back to the utility in some sort of net metering agreement. Solar trees are arrays that, as the name implies, mimic the look of trees, provide shade, and at night can function as street lights. In agricultural settings, the array may be used to directly power DC pumps, without the need for an inverter. In remote settings such as mountainous areas, islands, or other places where a power grid is unavailable, solar arrays can be used as the sole source of electricity, usually by charging a storage battery.



Fig: 2-18. Solar cell array on roof top

There is financial support available for people wishing to install PV arrays. In the UK, households are paid a 'Feed-in Tariff' to buy excess electricity at a flat rate per kWh. This is up to 44.3p/kWh which can allow a home to earn double their usual annual domestic electricity bill. The current UK feed-in tariff system is due for review on 31 March 2012, after which the current scheme may no longer be available.

2.2.6 Power Plants

A *photovoltaic power station* is a power station using photovoltaic modules and inverters for utility scale electricity generation, connected to an electricity transmission grid. Some large photovoltaic power stations like Waldpolenz Solar Park cover a significant area and have a maximum power output of 40-60 MW.¹



Fig: 2-19. Waldpolenz Solar Park, Germany

2.2.7 Connection to a DC grid

DC grids are only to be found in electric powered transport: railways trams and trolleybuses. A few pilot plants for such applications have been built, such as the tram depots in Hannover

Leinhausen and Geneva (Bachet de Pesay). The 150 kW_p Geneva site feeds 600V DC directly into the tram/trolleybus electricity network provided about 15% of the electricity at its opening in 1999.

2.2.8 Hybrid systems

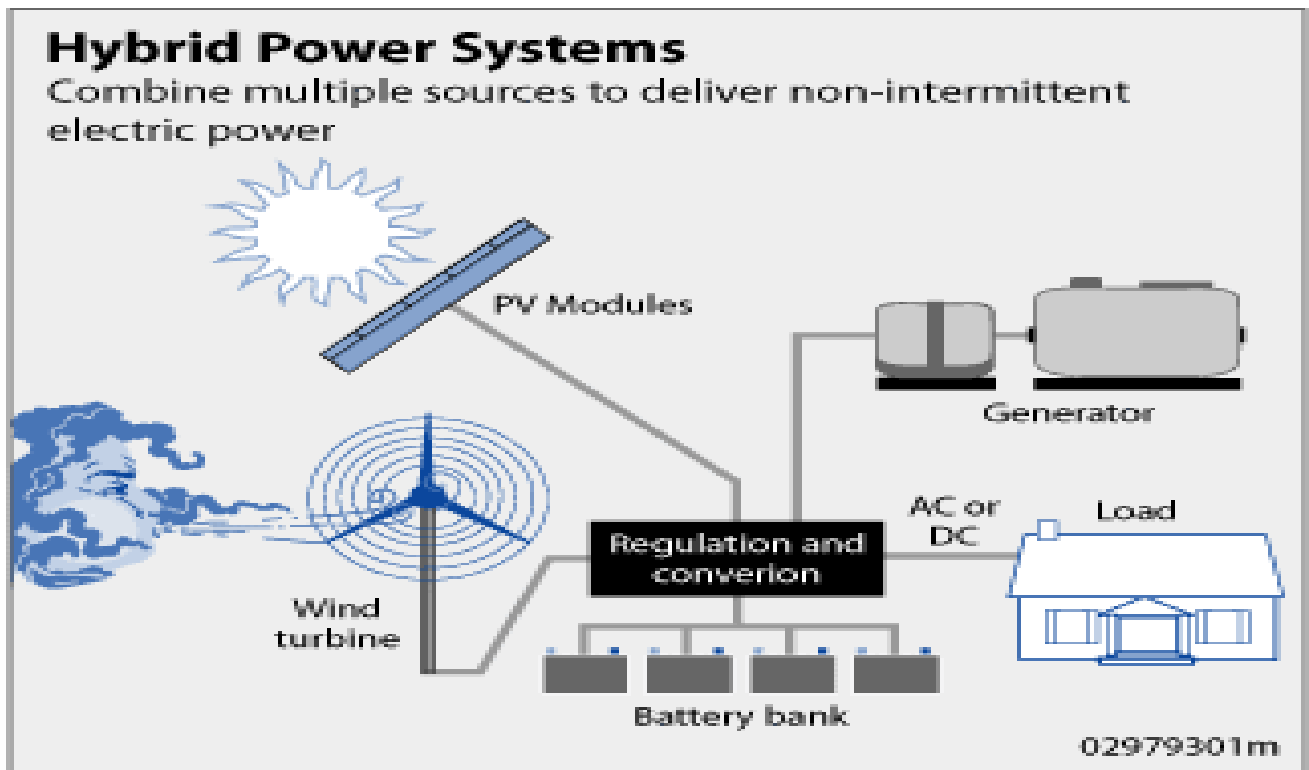


Fig: 2-20. Hybrid system

A hybrid system combines PV with other forms of generation, usually a diesel generator. Biogas is also used. The other form of generation may be a type able to modulate power output as a function of demand. However more than one renewable form of energy may be used e.g. wind. The photovoltaic power generation serves to reduce the consumption of non renewable fuel. Hybrid systems are most often found on islands. Pellworm island in Germany and Kythnos island in Greece are notable examples (both are combined with wind).^{[18][19]} The Kythnos plant has diocane diesel consumption by 11.2% .

There has also been recent work showing that the PV penetration limit can be increased by deploying a distributed network of PV+CHP hybrid systems in the U.S.^[21] The temporal distribution of solar flux, electrical and heating requirements for representative U.S. single family residences were analyzed and the results clearly show that hybridizing CHP with PV can enable additional PV deployment above what is possible with a conventional centralized electric generation system. This theory was reconfirmed with numerical simulations using per second solar flux data to determine that the necessary battery backup to provide for such a hybrid system is possible with relatively small and inexpensive battery systems.^[22] In addition, large PV+CHP systems are possible for institutional buildings, which again provide back up for intermittent PV and reduce CHP runtime.

2.2.9 Solar powered spacecraft

Solar energy is often used to supply power for satellites and spacecraft operating in the inner solar system since it can supply energy for a long time without excess fuel mass. A Communications satellite contains multiple radio transmitters which operate continually during its life. It would be uneconomic to operate such a vehicle (which may be on-orbit for years) from primary batteries or fuel cells, and refuelling in orbit is not practical. Solar power is not generally used to adjust the satellite's position, however, and the useful life of a communications satellite will be limited by the on-board station-keeping fuel supply.



Fig: 2-21. PV on the International Space Station

2.2.10 Solar Propelled Spacecraft

A few spacecraft operating within the orbit of Mars have used solar power as an energy source for their propulsion system.

All current solar powered spacecraft use solar panels in conjunction with electric propulsion, typically ion drives as this gives a very high exhaust velocity, and reduces the propellant over that of a rocket by more than a factor of ten. Since propellant is usually the biggest mass on many spacecraft, this reduces launch costs.

Other proposals for solar spacecraft include solar thermal heating of propellant, typically hydrogen or sometimes water is proposed. An electrodynamic tether can be used to change a satellite's orientation or adjust its orbit.

Another concept for solar propulsion in space is the light sail; this doesn't require conversion of light to electrical energy, instead relying directly on the tiny but persistent radiation pressure of light.

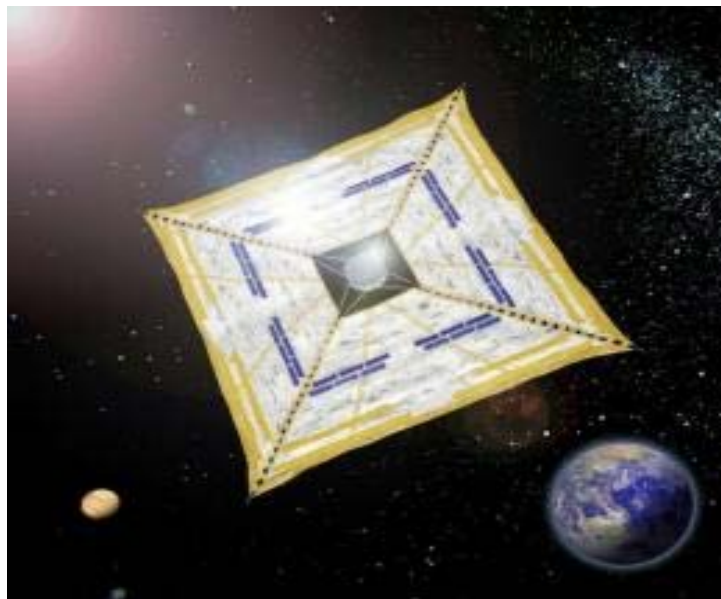


Fig: 2-22. Solar Propelled Spacecraft

2.3 Solar Cell Demand

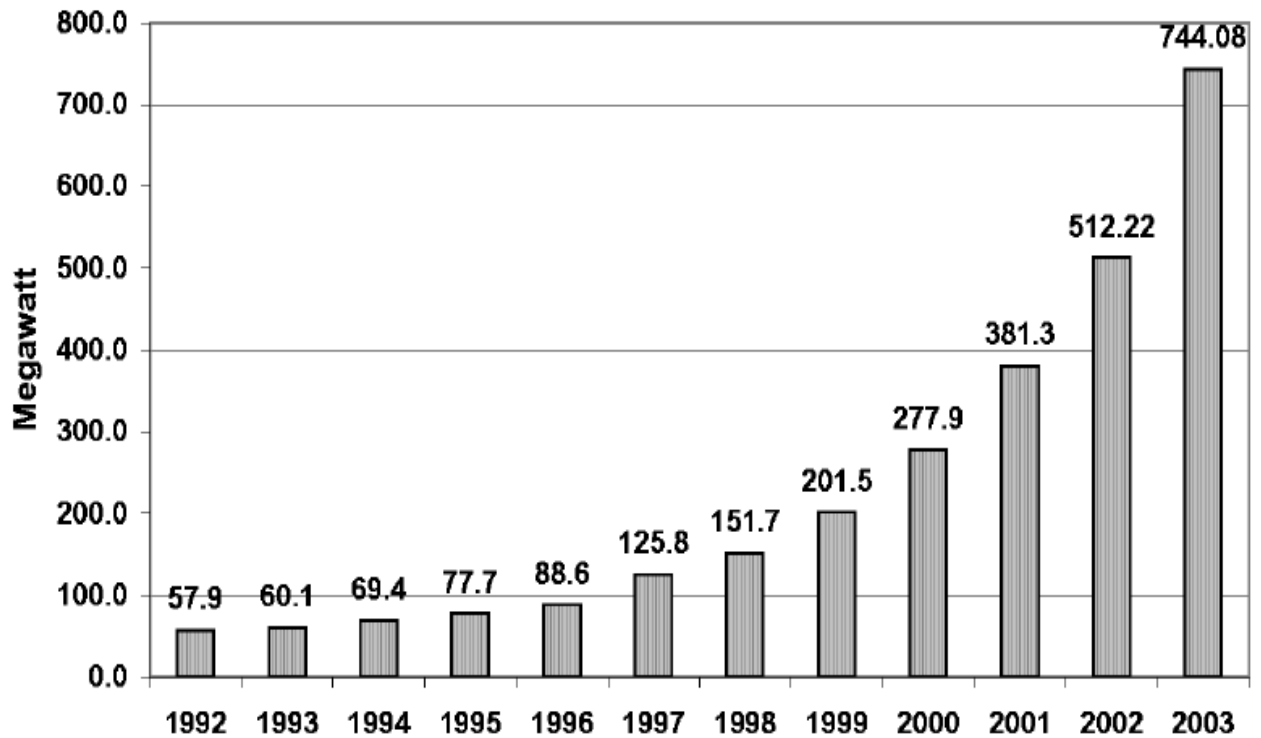


Fig: 2-23. Development of PV world market in MW_{peak} (MW_{peak} is defined as power under full sun, approx 1kW/m²)

GBI Research, a private company selling reports it calls "global business intelligence", projects thin film production to grow 24% from 2009 levels and to reach 22,214 MW in 202.

CHAPTER 3

MATERIAL PROPERTIES AND SOLAR CELL EFFICIENCY

3.1 Properties of Material

Different materials display different efficiencies and have different costs. Materials for efficient solar cells must have characteristics matched to the spectrum of available light. Some cells are designed to efficiently convert wavelengths of solar light that reach the Earth surface. However, some solar cells are optimized for light absorption beyond Earth's atmosphere as well. Light absorbing materials can often be used in *multiple physical configurations* to take advantage of different light absorption and charge separation mechanisms.

Materials presently used for photovoltaic solar cells include monocrystalline silicon, polycrystalline silicon, amorphous silicon, cadmium telluride, and copper indium selenide/sulfide.

Many currently available solar cells are made from bulk materials that are cut into wafers between 180 to 240 micrometers thick that are then processed like other semiconductors.

Other materials are made as thin-films layers, organic dyes, and organic polymers that are deposited on supporting substrates. A third group are made from nanocrystals and used as quantum dots (electron-confined nanoparticles). Silicon remains the only material that is well-researched in both *bulk* and *thin-film* forms.

3.1.1 Crystalline silicon

By far, the most prevalent *bulk* material for solar cells is crystalline silicon (abbreviated as a group as *c-Si*), also known as "solar grade silicon". Bulk silicon is separated into multiple categories according to crystallinity and crystal size in the resulting ingot, ribbon, or wafer.

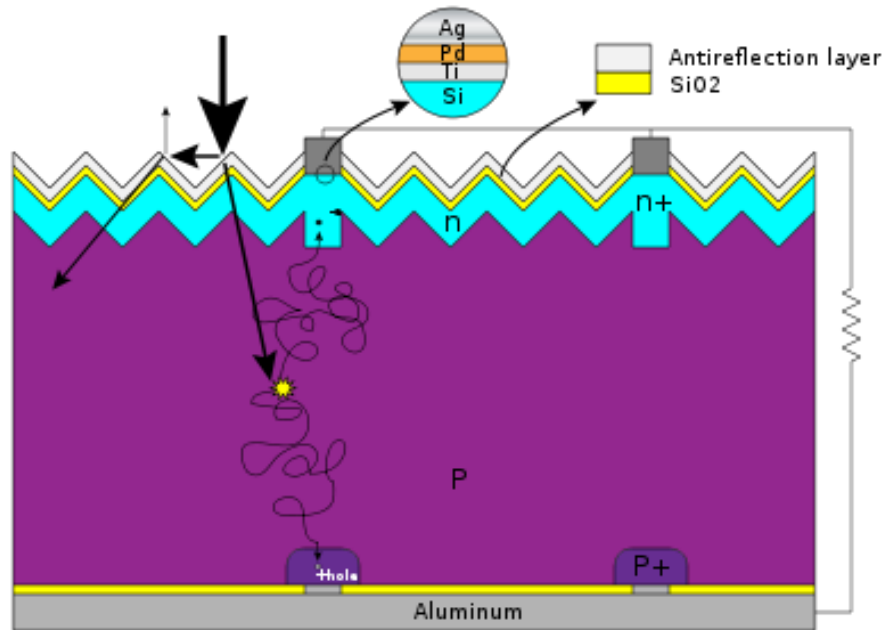


Fig: 3-1. Basic structure of a silicon based solar cell and its working mechanism.

1. **Monocrystalline silicon (c-Si):** often made using the Czochralski process. Single-crystal wafer cells tend to be expensive, and because they are cut from cylindrical ingots, do not completely cover a square solar cell module without a substantial waste of refined silicon. Hence most *c-Si* panels have uncovered gaps at the four corners of the cells.

2. **Polycrystalline silicon, or multicrystalline silicon, (poly-Si or mc-Si):** made from cast square ingots — large blocks of molten silicon carefully cooled and solidified. *Poly-Si* cells are less expensive to produce than single crystal silicon cells, but are less efficient. United States Department of Energy data show that there were a higher number of polycrystalline sales than monocrystalline silicon sales.

3. **Ribbon silicon is a type of polycrystalline silicon:** it is formed by drawing flat thin films from molten silicon and results in a polycrystalline structure. These cells

have lower efficiencies than poly-Si, but save on production costs due to a great reduction in silicon waste, as this approach does not require sawing from ingots.

Analysts have predicted that prices of polycrystalline silicon will drop as companies build additional polysilicon capacity quicker than the industry's projected demand. On the other hand, the cost of producing upgraded metallurgical-grade silicon, also known as UMG Si, can potentially be one-sixth that of making polysilicon.

Manufacturers of wafer-based cells have responded to high silicon prices in 2004-2008 prices with rapid reductions in silicon consumption. According to Jef Poortmans, director of IMEC's organic and solar department, current cells use between eight and nine grams of silicon per watt of power generation, with wafer thicknesses in the neighborhood of 0.200 mm. At 2008 spring's IEEE Photovoltaic Specialists' Conference (PVS'08), John Wohlgemuth, staff scientist at BP Solar, reported that his company has qualified modules based on 0.180 mm thick wafers and is testing processes for 0.16 mm wafers cut with 0.1 mm wire. IMEC's road map, presented at the organization's recent annual research review meeting, envisions use of 0.08 mm wafers by 2015.

3.1.2 Thin films

A **thin-film solar cell** (TFSC), also called a **thin-film photovoltaic cell** (TFPV), is a solar cell that is made by depositing one or more thin layers (thin film) of photovoltaic material on a substrate. The thickness range of such a layer is wide and varies from a few nanometers to tens of micrometers.

Many different photovoltaic materials are deposited with various deposition methods on a variety of substrates. Thin-film solar cells are usually categorized according to the photovoltaic material used:

- Amorphous silicon (a-Si) and other thin-film silicon (TF-Si)
- Cadmium Telluride (CdTe)
- Copper indium gallium selenide (CIS or CIGS)
- Dye-sensitized solar cell (DSC) and other organic solar cell

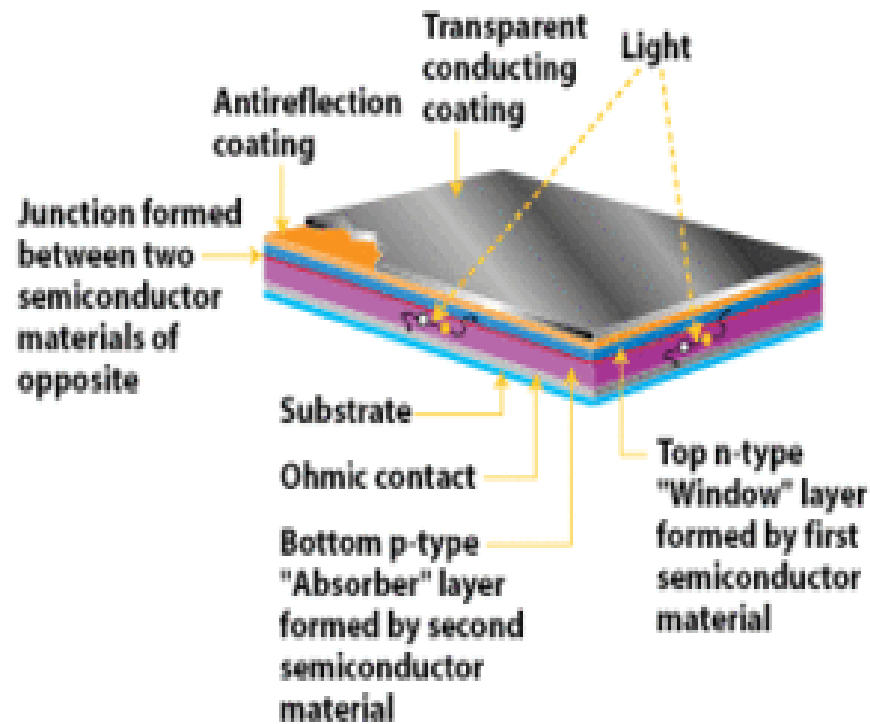


Fig: 3-2. Cross-section of thin film polycrystalline solar cell

In 2010 the market share of thin film declined by 30% as thin film technology was displaced by more efficient crystalline silicon solar panels (the light and dark blue bars).

Thin-film technologies reduce the amount of material required in creating the active material of solar cell. Most thin film solar cells are sandwiched between two panes of glass to make a module.

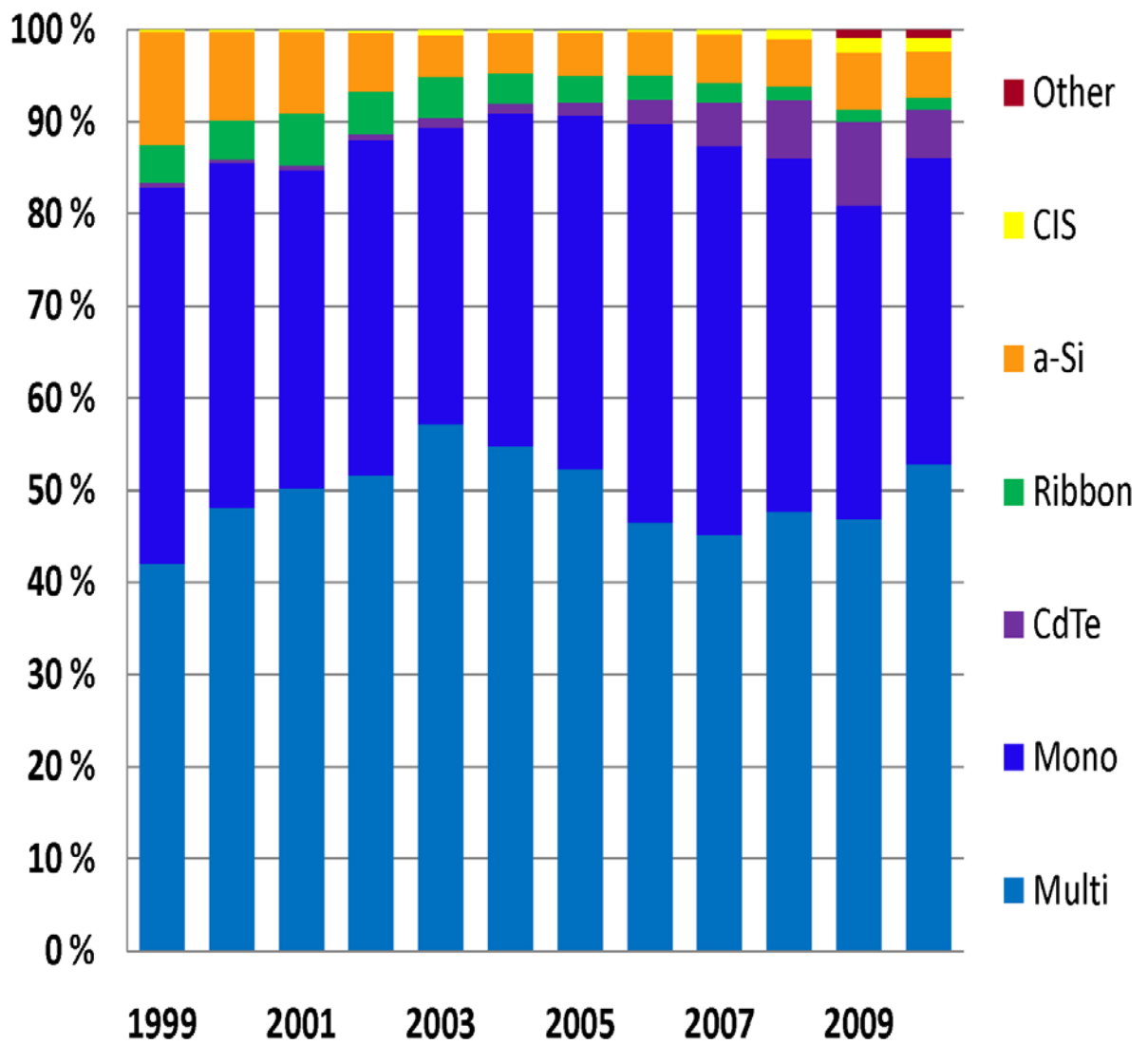


Fig: 3-3. Market share of the different PV technologies

Since silicon solar panels only use one pane of glass, thin film panels are approximately twice as heavy as crystalline silicon panels. The majority of film panels have significantly lower conversion efficiencies, lagging silicon by two to three percentage points. Thin-film solar

technologies have enjoyed large investment due to the success of First Solar and the largely unfulfilled promise of lower cost and flexibility compared to wafer silicon cells, but they have not become mainstream solar products due to their lower efficiency and corresponding larger area consumption per watt production. Cadmium telluride (CdTe), copper indium gallium selenide (CIGS) and amorphous silicon (A-Si) are three thin-film technologies often used as outdoor photovoltaic solar power production. CdTe technology is most cost competitive among them. CdTe technology costs about 30% less than CIGS technology and 40% less than A-Si technology in 2011.

3.1.2.1 Cadmium Telluride Solar Cell

A cadmium telluride solar cell uses a cadmium telluride (CdTe) thin film, a semiconductor layer to absorb and convert sunlight into electricity. Solarbuzz has reported that the lowest quoted thin-film module price stands at US\$1.76 per watt-peak, with the lowest crystalline silicon (c-Si) module at \$2.48 per watt-peak.

The cadmium present in the cells would be toxic if released. However, release is impossible during normal operation of the cells and is unlikely during fires in residential roofs. A square meter of CdTe contains approximately the same amount of Cd as a single C cell Nickel-cadmium battery, in a more stable and less soluble form.

3.1.2.2 Copper Indium Gallium Selenide

Copper indium gallium selenide (CIGS) is a direct band gap material. It has the highest efficiency (~20%) among thin film materials (see CIGS solar cell). Traditional methods of fabrication involve vacuum processes including co-evaporation and sputtering. Recent developments at IBM and Nanosolar attempt to lower the cost by using non-vacuum solution processes.

Properties

CIGS is a I-III-VI₂ compound semiconductor material composed of copper, indium, gallium, and selenium. The material is a solid solution of copper indium selenide (often abbreviated "CIS") and copper gallium selenide, with a chemical formula of $\text{CuIn}_x\text{Ga}_{(1-x)}\text{Se}_2$, where the value of x can vary from 1 (pure copper indium selenide) to 0 (pure copper gallium selenide). It is a tetrahedrally bonded semiconductor, with the chalcopyrite crystal structure. The bandgap varies continuously with x from about 1.0 eV (for copper indium selenide) to about 1.7 eV (for copper gallium selenide).

CIGS has an exceptionally high absorption coefficient of more than $10^5/\text{cm}$ for 1.5 eV and higher energy photons.^[3] CIGS solar cells with efficiencies greater than 20% have been claimed by both the National Renewable Energy Laboratory (NREL) and the Zentrum für Sonnenenergie und Wasserstoff Forschung (ZSW), which is the record to date for any thin film solar cell.

3.1.2.3 CIGS Photovoltaic Cells

The most common device structure for CIGS solar cells is shown in Figure 2. Glass is commonly used as a substrate, however, many companies are also looking at lighter and more flexible substrates such as polyimide or metal foils.^[6] A molybdenum layer is deposited (commonly by sputtering) which serves as the back contact and to reflect most unabsorbed light back into the absorber. Following Mo deposition a p-type CIGS absorber layer is grown by one of several unique methods. A thin n-type buffer layer is added on top of the absorber. The buffer is typically CdS deposited via chemical bath deposition. The buffer is overlaid with a thin, intrinsic ZnO layer which is capped by a thicker, Al doped ZnO layer. Despite increasing the series resistance, the intrinsic ZnO layer is beneficial to cell performance. The precise mechanism for the improvement is still being debated.^[7] The Al doped ZnO serves as a transparent conducting oxide to collect and move electrons out of the cell while absorbing as little light as possible.

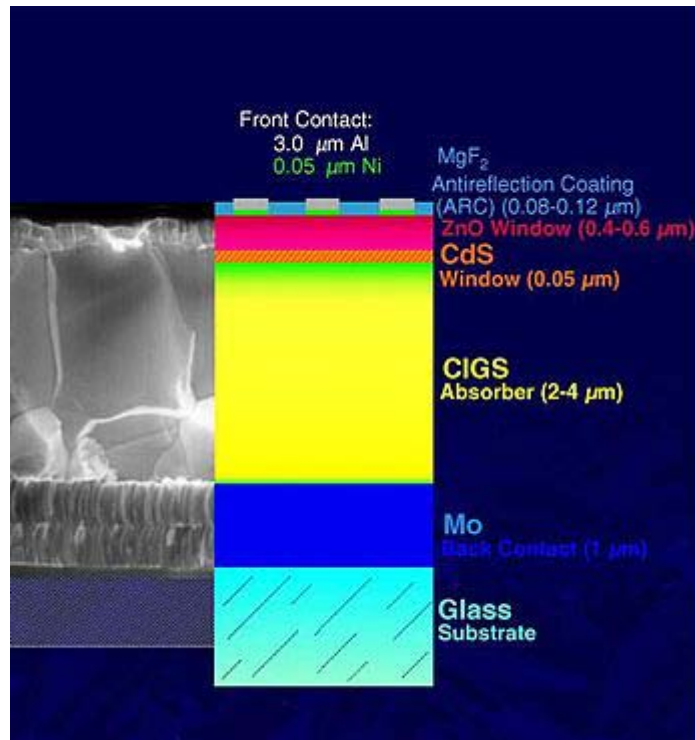


Fig: 3-4. CIGS device structure

The materials based on CuInSe_2 that are of interest for photovoltaic applications include several elements from groups I, III and VI in the periodic table. These semiconductors are especially attractive for thin film solar cell application because of their high optical absorption coefficients and versatile optical and electrical characteristics which can in principle be manipulated and tuned for a specific need in a given device.^[8]

3.1.2.4 General Properties of High Performance CIGS Absorbers

All high performance CIGS absorbers in solar cells have several similarities independent of the growth technique used. First, they are polycrystalline α -phase which has the chalcopyrite crystal structure shown in Figure 3. The second property is an overall Cu deficiency.^[20] Cu deficiency increases the majority carrier (hole) concentration by increasing the number of Cu vacancies. These vacancies act as electron acceptors. Also, when CIGS films are In rich (Cu deficient) the surface layer of the film forms an ordered defect compound (ODC) with a

stoichiometry of $\text{Cu}(\text{In,Ga})_3\text{Se}_5$. The ODC is n-type, forming a p-n homojunction in the film at the interface between the α phase and the ODC. Recombination velocity at the CIGS/CdS interface is decreased by presence of the homojunction. The drop in interface recombination attributable to ODC formation is demonstrated by experiments which have shown recombination in the bulk of the film is the main loss mechanism in Cu deficient films, while in Cu rich films the main loss is at the CIGS/CdS interface.^{[7][20]}

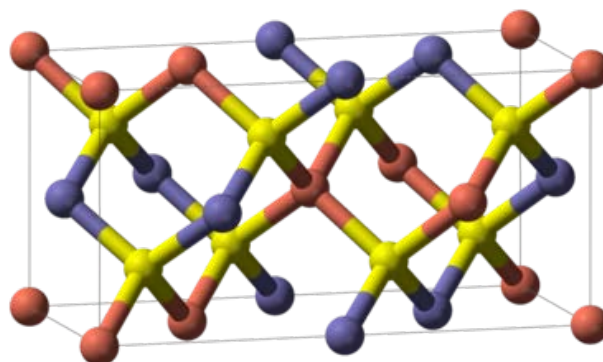


Fig: 3-5: CIGS unit cell. Red = Cu, Yellow = Se, Blue = In/Ga

Sodium (Na) incorporation is also necessary for optimal performance. Ideal Na concentration is considered to be approximately 0.1 at%. Na is commonly supplied by the soda-lime glass used as the substrate, but in processes that do not use this substrate the Na must be deliberately added. Beneficial effects of Na include increases in p-type conductivity, texture, and average grain size. Furthermore, Na incorporation allows for performance to be maintained over larger stoichiometric deviations.^[3] Simulations have predicted that Na on an In site creates a shallow acceptor level and that Na serves to remove In on Cu defects (donors), but reasons for these benefits are still being debated. Na is also credited with catalyzing oxygen absorption. Oxygen passivates Se vacancies that act as compensating donors and recombination centers.

Alloying CIS (CuInSe_2) with CGS (CuGaSe_2) increases in the bandgap. To reach the ideal bandgap for a single junction solar cell, 1.5 eV, a $\text{Ga}/(\text{In}+\text{Ga})$ ratio of roughly 0.7 would be optimal. However, at ratios above ~ 0.3 device performance drops off. Industry currently targets the 0.3 $\text{Ga}/(\text{In}+\text{Ga})$ ratio, resulting in bandgaps between 1.1 and 1.2 eV. The

decreasing performance has been postulated to be a result of CGS not forming the ODC, which is necessary for a good interface with CdS.

The highest efficiency devices show a high degree of texturing, or preferred crystallographic orientation. Until recently record efficiency devices displayed a (112) texture, but now a (204) surface orientation is observed in the best quality devices.^[3] A smooth absorber surface is preferred to maximize the ratio of the illuminated area to the area of the interface. The area of the interface increases with roughness while illuminated area remains constant, decreasing open circuit voltage (V_{OC}). Studies have also linked an increase in defect density to decreased V_{OC} . recombination in CIGS has been suggested to be dominated by non-radiative processes. Theoretically, recombination can be controlled by engineering of the film, as opposed to being intrinsic to the material.

3.1.2.5 Gallium Arsenide Multijunction

High-efficiency multijunction cells were originally developed for special applications such as satellites and space exploration, but at present, their use in terrestrial concentrators might be the lowest cost alternative in terms of \$/kWh and \$/W. These multijunction cells consist of multiple thin films produced using metalorganic vapour phase epitaxy. A triple-junction cell, for example, may consist of the semiconductors: GaAs, Ge, and GaInP₂. Each type of semiconductor will have a characteristic band gap energy which, loosely speaking, causes it to absorb light most efficiently at a certain color, or more precisely, to absorb electromagnetic radiation over a portion of the spectrum. The semiconductors are carefully chosen to absorb nearly all of the solar spectrum, thus generating electricity from as much of the solar energy as possible.

GaAs based multijunction devices are the most efficient solar cells to date. In October 2010, triple junction metamorphic cell reached a record high of 42.3%. This technology is currently being utilized in the Mars Exploration Rover missions, which have run far past their 90 day design life.

Tandem solar cells based on monolithic, series connected, gallium indium phosphide (GaInP), gallium arsenide GaAs, and germanium Ge p-n junctions, are seeing demand rapidly rise. Between December 2006 and December 2007, the cost of 4N gallium metal rose from about \$350 per kg to \$680 per kg. Additionally, germanium metal prices have risen substantially to \$1000–\$1200 per kg this year. Those materials include gallium (4N, 6N and 7N Ga), arsenic (4N, 6N and 7N) and germanium, pyrolytic boron nitride (pBN) crucibles for growing crystals, and boron oxide, these products are critical to the entire substrate manufacturing industry.

Triple-junction GaAs solar cells were also being used as the power source of the Dutch four-time World Solar Challenge winners Nuna in 2003, 2005 and 2007, and also by the Dutch solar cars Solutra (2005), Twente One (2007) and 21Revolution (2009).

The Dutch Radboud University Nijmegen set the record for thin film solar cell efficiency using a single junction GaAs to 25.8% in August 2008 using only 4 μm thick GaAs layer which can be transferred from a wafer base to glass or plastic film.

3.1.2.6 Light-Absorbing Dyes (DSSC)

Dye-sensitized solar cells (DSSCs) are made of low-cost materials and do not need elaborate equipment to manufacture, so they can be made in a DIY fashion, possibly allowing players to produce more of this type of solar cell than others. In bulk it should be significantly less expensive than older solid-state cell designs. DSSC's can be engineered into flexible sheets, and although its conversion efficiency is less than the best thin film cells, its price/performance ratio should be high enough to allow them to compete with fossil fuel electrical generation. The DSSC has been developed by Prof. Michael Grätzel in 1991 at the Swiss Federal Institute of Technology (EPFL) in Lausanne (CH).

Typically a ruthenium metalorganic dye (Ru-centered) is used as a monolayer of light-absorbing material. The dye-sensitized solar cell depends on a mesoporous layer of nanoparticulate titanium dioxide to greatly amplify the surface area (200–300 m^2/g TiO_2 , as compared to approximately 10 m^2/g of flat single crystal). The photogenerated electrons from

the *light absorbing dye* are passed on to the *n-type* TiO₂, and the holes are absorbed by an electrolyte on the other side of the dye. The circuit is completed by a redox couple in the electrolyte, which can be liquid or solid. This type of cell allows a more flexible use of materials, and is typically manufactured by screen printing and/or use of Ultrasonic Nozzles, with the potential for lower processing costs than those used for *bulk* solar cells. However, the dyes in these cells also suffer from degradation under heat and UV light, and the cell casing is difficult to seal due to the solvents used in assembly. In spite of the above, this is a popular emerging technology with some commercial impact forecast within this decade. The first commercial shipment of DSSC solar modules occurred in July 2009 from G24i Innovations.

3.1.2.7 Organic/Polymer Solar Cells

Organic solar cells are a relatively novel technology, yet hold the promise of a substantial price reduction (over thin-film silicon) and a faster return on investment. These cells can be processed from solution, hence the possibility of a simple roll-to-roll printing process, leading to inexpensive, large scale production.

Organic solar cells and polymer solar cells are built from thin films (typically 100 nm) of organic semiconductors including polymers, such as polyphenylene vinylene and small-molecule compounds like copper phthalocyanine (a blue or green organic pigment) and carbon fullerenes and fullerene derivatives such as PCBM. Energy conversion efficiencies achieved to date using conductive polymers are low compared to inorganic materials. However, it has improved quickly in the last few years and the highest NREL (National Renewable Energy Laboratory) certified efficiency has reached 8.3% for the Konarka Power Plastic. In addition, these cells could be beneficial for some applications where mechanical flexibility and disposability are important.

These devices differ from inorganic semiconductor solar cells in that they do not rely on the large built-in electric field of a PN junction to separate the electrons and holes created when photons are absorbed. The active region of an organic device consists of two materials, one which acts as an electron donor and the other as an acceptor. When a photon is converted into an electron hole pair, typically in the donor material, the charges tend to remain bound in the

form of an exciton, and are separated when the exciton diffuses to the donor-acceptor interface. The short exciton diffusion lengths of most polymer systems tend to limit the efficiency of such devices. Nanostructured interfaces, sometimes in the form of bulk heterojunctions, can improve performance.

3.1.2.8 Silicon Thin Films

Silicon thin-film cells are mainly deposited by chemical vapor deposition (typically plasma-enhanced, PE-CVD) from silane gas and hydrogen gas. Depending on the deposition parameters, this can yield.

1. Amorphous silicon (a-Si or a-Si:H)
2. Protocrystalline silicon or
3. Nanocrystalline silicon (nc-Si or nc-Si:H), also called microcrystalline silicon.

It has been found that protocrystalline silicon with a low volume fraction of nanocrystalline silicon is optimal for high open circuit voltage. These types of silicon present dangling and twisted bonds, which results in deep defects (energy levels in the bandgap) as well as deformation of the valence and conduction bands (band tails). The solar cells made from these materials tend to have lower *energy conversion efficiency* than *bulk* silicon, but are also less expensive to produce. The quantum efficiency of thin film solar cells is also lower due to reduced number of collected charge carriers per incident photon.

An amorphous silicon (a-Si) solar cell is made of amorphous or microcrystalline silicon and its basic electronic structure is the p-i-n junction. a-Si is attractive as a solar cell material because it is abundant and non-toxic (unlike its CdTe counterpart) and requires a low processing temperature, enabling production of devices to occur on flexible and low-cost substrates. As the amorphous structure has a higher absorption rate of light than crystalline cells, the complete light spectrum can be absorbed with a very thin layer of photo-electrically active material. A film only 1 micron thick can absorb 90% of the usable solar energy. This reduced material requirement along with current technologies being capable of large-area deposition of a-Si, the scalability of this type of cell is high. However, because it is

amorphous, it has high inherent disorder and dangling bonds, making it a bad conductor for charge carriers. These dangling bonds act as recombination centers that severely reduce the carrier lifetime and pin the Fermi energy level so that doping the material to n- or p- type is not possible. Amorphous Silicon also suffers from the Staebler-Wronski effect, which results in the efficiency of devices utilizing amorphous silicon dropping as the cell is exposed to light. The production of a-Si thin film solar cells uses glass as a substrate and deposits a very thin layer of silicon by plasma-enhanced chemical vapor deposition (PECVD). A-Si manufacturers are working towards lower costs per watt and higher conversion efficiency with continuous research and development on Multijunction solar cells for solar panels. An well Technologies Limited recently announced its target for multi-substrate-multi-chamber PECVD, to lower the cost to US\$0.5 per watt.

Amorphous silicon has a higher bandgap (1.7 eV) than crystalline silicon (c-Si) (1.1 eV), which means it absorbs the visible part of the solar spectrum more strongly than the infrared portion of the spectrum. As **nc-Si** has about the same bandgap as c-Si, the nc-Si and a-Si can advantageously be combined in thin layers, creating a layered cell called a **tandem cell**. The top cell in a-Si absorbs the visible light and leaves the infrared part of the spectrum for the bottom cell in nc-Si.

Recently, solutions to overcome the limitations of thin-film crystalline silicon have been developed. Light trapping schemes where the weakly absorbed long wavelength light is obliquely coupled into the silicon and traverses the film several times can significantly enhance the absorption of sunlight in the thin silicon films.^[19] Minimizing the top contact coverage of the cell surface is another method for reducing optical losses; this approach simply aims at reducing the area that is covered over the cell to allow for maximum light input into the cell. Anti-reflective coatings can also be applied to create destructive interference within the cell. This can be done by modulating the Refractive index of the surface coating; if destructive interference is achieved, there will be no reflective wave and thus all light will be transmitted into the semiconductor cell. Surface texturing is another option, but may be less viable because it also increases the manufacturing price. By applying a texture to the surface of the solar cell, the reflected light can be refracted into striking the surface again, thus reducing the overall light reflected out. Light trapping as another method

allows for a decrease in overall thickness of the device; the path length that the light will travel is several times the actual device thickness. This can be achieved by adding a textured backreflector to the device as well as texturing the surface. If both front and rear surfaces of the device meet this criterion, the light will be 'trapped' by not having an immediate pathway out of the device due to internal reflections. Thermal processing techniques can significantly enhance the crystal quality of the silicon and thereby lead to higher efficiencies of the final solar cells.^[10] Further advancement into geometric considerations of building devices can exploit the dimensionality of nanomaterials. Creating large, parallel nanowire arrays enables long absorption lengths along the length of the wire while still maintaining short minority carrier diffusion lengths along the radial direction. Adding nanoparticles between the nanowires will allow for conduction through the device. Because of the natural geometry of these arrays, a textured surface will naturally form which allows for even more light to be trapped. A further advantage of this geometry is that these types of devices require about 100 times less material than conventional wafer-based devices.

3.2 Efficiency of Solar Cell

The **efficiency** of a **solar cell** may be broken down into reflectance efficiency, thermodynamic efficiency, charge carrier separation efficiency and conductive efficiency. The overall efficiency is the product of each of these individual efficiencies.

Due to the difficulty in measuring these parameters directly, other parameters are measured instead: thermodynamic efficiency, quantum efficiency, V_{OC} ratio, and fill factor. Reflectance losses are a portion of the quantum efficiency under "external quantum efficiency". Recombination losses make up a portion of the quantum efficiency, V_{OC} ratio, and fill factor. Resistive losses are predominantly categorized under fill factor, but also make up minor portions of the quantum efficiency, V_{OC} ratio.

3.2.1 Energy Conversion Efficiency

Energy conversion efficiency is **the ratio between the useful output of an energy conversion machine and the input, in energy terms. The useful output may be electric power, mechanical work, or heat.**

A solar cell's *energy conversion efficiency* (η , "eta"), is the percentage of incident light energy that actually ends up as electric power. This is calculated at the maximum power point, P_m , divided by the input light *irradiance* (E , in W/m^2) under standard test conditions (STC) and the *surface area* of the solar cell (A_c in m^2).

$$\eta = \frac{P_m}{E \times A_c}$$

STC specifies a temperature of $25\text{ }^\circ\text{C}$ and an irradiance of $1000\text{ W}/\text{m}^2$ with an air mass 1.5 (AM1.5) spectrum. These correspond to the irradiance and spectrum of sunlight incident on a clear day upon a sun-facing 37° -tilted surface with the sun at an angle of 41.81° above the horizon.^{[1][2]} This condition approximately represents solar noon near the spring and autumn equinoxes in the continental United States with surface of the cell aimed directly at the sun. For example, under these test conditions a solar cell of 12% efficiency with a 100 cm^2 (0.01 m^2) surface area would produce 1.2 watts of power.

3.2.2 Thermodynamic Efficiency Limit

The Shockley-Queisser limit for the theoretical maximum efficiency of a solar cell. Semiconductors with band gap between 1 and 1.5eV have the greatest potential to form an efficient cell. . This calculated curve uses actual solar spectrum data, and therefore the curve is wiggly from IR absorption bands in the atmosphere. This efficiency limit of ~34% can be exceeded by multijunction solar cells.

The absolute maximum theoretically possible conversion efficiency for sunlight is about 95% due to the Carnot limit, given the temperature of the photons emitted by the Sun's surface.

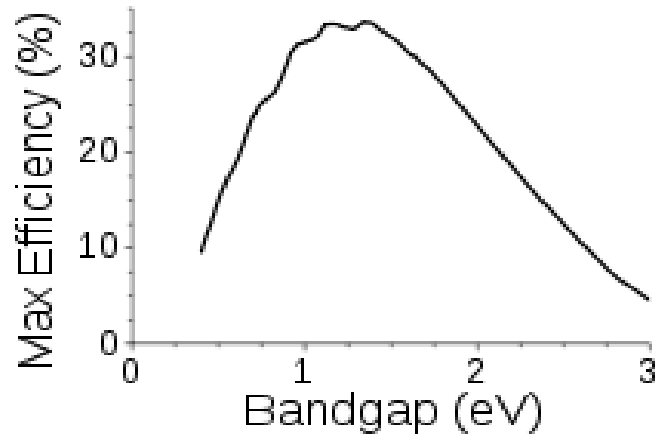


Fig: 3-6. Efficiency vs Bandgap energy

However, solar cells operate as quantum energy conversion devices, and are therefore subject to the "thermodynamic efficiency limit". Photons with an energy below the band gap of the absorber material cannot generate a hole-electron pair, and so their energy is not converted to useful output and only generates heat if absorbed. For photons with an energy above the band gap energy, only a fraction of the energy above the band gap can be converted to useful output. When a photon of greater energy is absorbed, the excess energy above the band gap is converted to kinetic energy of the carrier combination. The excess kinetic energy is converted to heat through phonon interactions as the kinetic energy of the carriers slows to equilibrium velocity.

Solar cells with multiple band gap absorber materials improve efficiency by dividing the solar spectrum into smaller bins where the thermodynamic efficiency limit is higher for each bin.

3.2.3 Quantum Efficiency

As described above, when a photon is absorbed by a solar cell it can produce an electron-hole pair. One of the carriers may reach the p-n junction and contribute to the current produced by the solar cell; such a carrier is said to be *collected*. Or, the carriers recombine with no net contribution to cell current.

Quantum efficiency refers to the percentage of photons that are converted to electric current (i.e., collected carriers) when the cell is operated under short circuit conditions. Some of the light striking the cell is reflected, or passes through the cell; external quantum efficiency is the fraction of incident photons that are converted to electric current. Not all the photons captured by the cell contribute to electric current; internal quantum efficiency (IQE) is the fraction of *absorbed* photons that are converted to electric current. Thick cells let through little light.

Quantum efficiency is most usefully expressed as a *spectral* measurement (that is, as a function of photon wavelength or energy). Since some wavelengths are absorbed more effectively than others, spectral measurements of quantum efficiency can yield valuable information about the quality of the semiconductor bulk and surfaces. Quantum efficiency alone is not the same as overall energy conversion efficiency, as it does not convey information about the fraction of power that is converted by the solar cell.

Types

A graph showing variation of internal quantum efficiency, external quantum efficiency, and reflectance with wavelength of a crystalline silicon solar cell.

Two types of **quantum efficiency (QE)** of a solar cell are often considered:

- **External Quantum Efficiency (EQE)** is the ratio of the number of charge carriers collected by the solar cell to the number of photons of a given energy *shining on the solar cell from outside* (incident photons).
- **Internal Quantum Efficiency (IQE)** is the ratio of the number of charge carriers collected by the solar cell to the number of photons of a given energy that shine on the solar cell from outside *and* are absorbed by the cell.

The IQE is always larger than the EQE. A low IQE indicates that the active layer of the solar cell is unable to make good use of the photons. A low EQE can indicate that, but it can also, instead, indicate that a lot of the light was reflected.

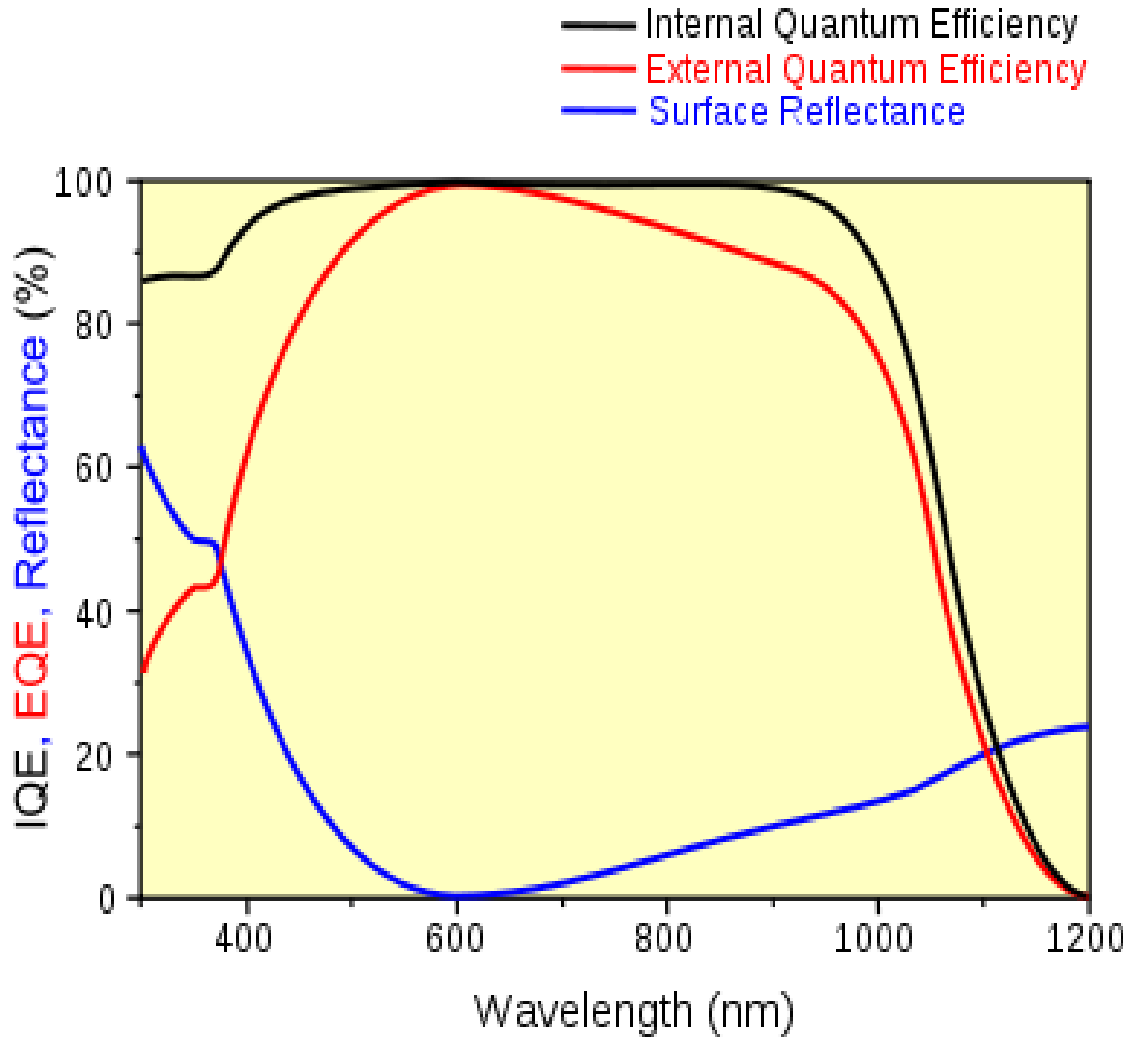


Fig: 3-7. IQE, EQE, Reflectance vs Wavelength

To measure the IQE, one first measures the EQE of the solar device, then measures its transmission and reflection, and combines these data to infer the IQE.

3.2.4 Maximum-power Point

A solar cell may operate over a wide range of voltages (V) and currents (I). By increasing the resistive load on an irradiated cell continuously from zero (a *short circuit*) to a very high

value (an *open circuit*) one can determine the maximum-power point, the point that maximizes $V \times I$; that is, the load for which the cell can deliver maximum electrical power at that level of irradiation. (The output power is zero in both the short circuit and open circuit extremes).

A high quality, monocrystalline silicon solar cell, at 25 °C cell temperature, may produce 0.60 volts open-circuit (V_{OC}). The cell temperature in full sunlight, even with 25 °C air temperature, will probably be close to 45 °C, reducing the open-circuit voltage to 0.55 volts per cell. The voltage drops modestly, with this type of cell, until the short-circuit current is approached (I_{SC}). Maximum power (with 45 °C cell temperature) is typically produced with 75% to 80% of the open-circuit voltage (0.43 volts in this case) and 90% of the short-circuit current. This output can be up to 70% of the $V_{OC} \times I_{SC}$ product. The short-circuit current (I_{SC}) from a cell is nearly proportional to the illumination, while the open-circuit voltage (V_{OC}) may drop only 10% with a 80% drop in illumination. Lower-quality cells have a more rapid drop in voltage with increasing current and could produce only 1/2 V_{OC} at 1/2 I_{SC} . The usable power output could thus drop from 70% of the $V_{OC} \times I_{SC}$ product to 50% or even as little as 25%. Vendors who rate their solar cell "power" only as $V_{OC} \times I_{SC}$, without giving load curves, can be seriously distorting their actual performance.

The maximum power point of a photovoltaic varies with incident illumination. For example, accumulation of dust on photovoltaic panels reduces the maximum power point^[5]. For systems large enough to justify the extra expense, a maximum power point tracker tracks the instantaneous power by continually measuring the voltage and current (and hence, power transfer), and uses this information to dynamically adjust the load so the maximum power is *always* transferred, regardless of the variation in lighting.

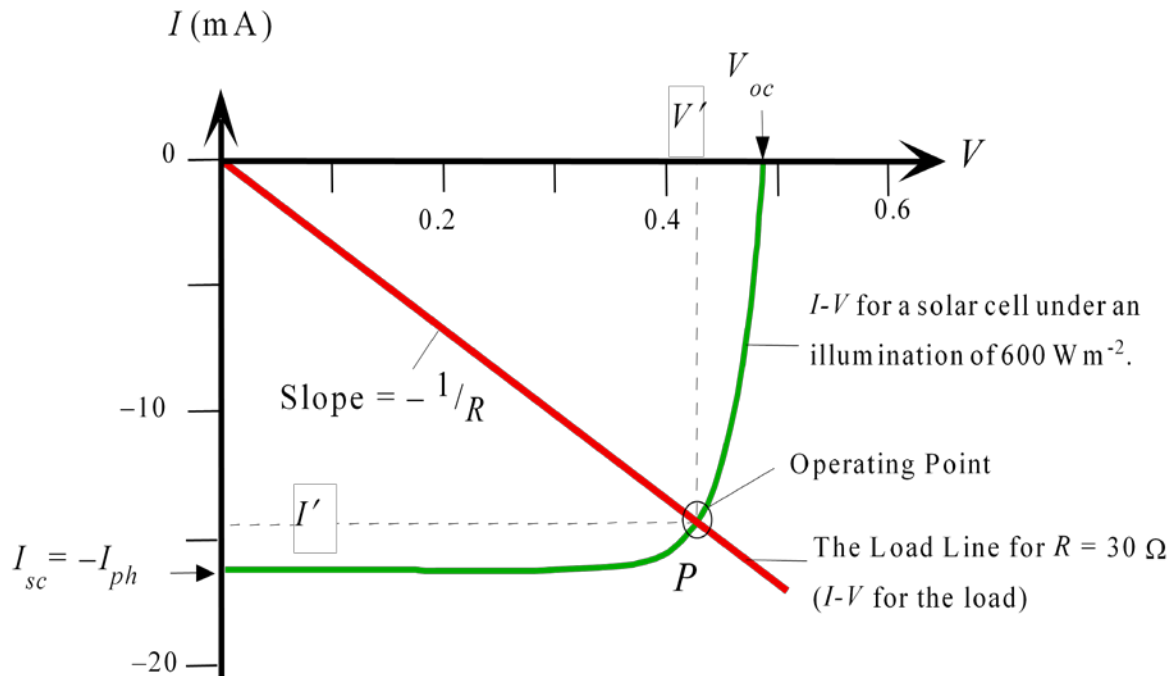


Fig-3.8- I-V characteristics curve

3.2.5 Fill Factor

Another defining term in the overall behavior of a solar cell is the *fill factor (FF)*. This is the ratio of the available power at the *maximum power point (P_m)* divided by the *open circuit voltage (V_{OC})* and the *short circuit current (I_{SC})*:

$$FF = \frac{P_m}{V_{OC} \times I_{SC}} = \frac{\eta \times A_c \times E}{V_{OC} \times I_{SC}}$$

The fill factor is directly affected by the values of the cell's series and shunt resistances. Increasing the shunt resistance (R_{sh}) and decreasing the series resistance (R_s) lead to a higher

fill factor, thus resulting in greater efficiency, and bringing the cell's output power closer to its theoretical maximum.

3.2.6 Comparison of Energy Conversion Efficiencies

Energy conversion efficiency is measured by dividing the electrical power produced by the cell by the light power falling on the cell. Many factors influence the electrical power output, including spectral distribution, spatial distribution of power, temperature, and resistive load applied to the cell. IEC standard 61215 is used to compare the performance of cells and is designed around terrestrial, temperate conditions, using its standard temperature and conditions (STC): irradiance of 1 kW/m^2 , a spectral distribution close to solar radiation through AM (airmass) of 1.5 and a cell temperature $25 \text{ }^\circ\text{C}$. The resistive load is varied until the peak or maximum power point (MPP) is achieved. The power at this point is recorded as Watt-peak (Wp). The same standard is used for measuring the power and efficiency of PV modules,

Air mass has an effect on power output. In space, where there is no atmosphere, the spectrum of the sun is relatively unfiltered. However, on earth with air filtering the incoming light, the solar spectrum changes. To account for the spectral differences, a system was devised to calculate this filtering effect. Simply, the filtering effect ranges from Air Mass 0 (AM0) in space, to approximately Air Mass 1.5 on Earth. Multiplying the spectral differences by the quantum efficiency of the solar cell in question will yield the efficiency of the device. For example, a silicon solar cell in space might have an efficiency of 14% at AM0, but have an efficiency of 16% on earth at AM 1.5. Terrestrial efficiencies typically are greater than space efficiencies.

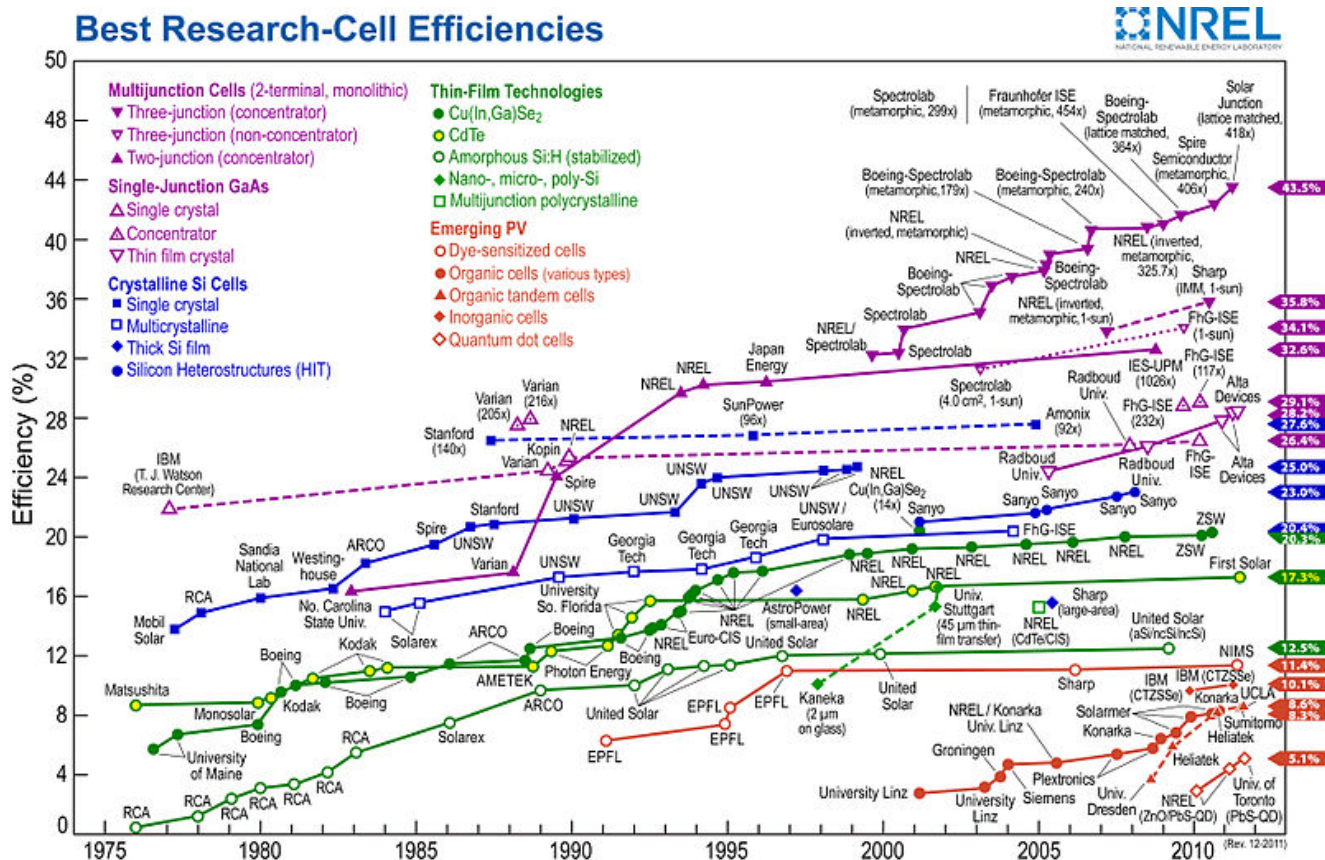


Fig: 3-9. Comparison of energy conversion efficiencies

Solar cell efficiencies vary from 6% for amorphous silicon-based solar cells to 40.7% with multiple-junction research lab cells and 42.8% with multiple dies assembled into a hybrid package.^[7] Solar cell energy conversion efficiencies for commercially available *multicrystalline Si* solar cells are around 14-19%.^[8] The highest efficiency cells have not always been the most economical — for example a 30% efficient multijunction cell based on exotic materials such as gallium arsenide or indium selenide and produced in low volume might well cost one hundred times as much as an 8% efficient amorphous silicon cell in mass production, while only delivering about four times the electrical power.

However, there is a way to "boost" solar power. By increasing the light intensity, typically photogenerated carriers are increased, resulting in increased efficiency by up to 15%. These so-called "concentrator systems" have only begun to become cost-competitive as a result of the development of high efficiency GaAs cells. The increase in intensity is typically

accomplished by using concentrating optics. A typical concentrator system may use a light intensity 6-400 times the sun, and increase the efficiency of a one sun GaAs cell from 31% at AM 1.5 to 35%. See Solar_cell#Concentrating photovoltaics (CPV) below and Concentrating solar power (CSP).

A common method used to express economic costs of electricity-generating systems is to calculate a price per delivered kilowatt-hour (kWh). The solar cell efficiency in combination with the available irradiation has a major influence on the costs, but generally speaking the overall system efficiency is important. Using the commercially available solar cells (as of 2006) and system technology leads to system efficiencies between 5 and 19%. As of 2005, photovoltaic electricity generation costs ranged from ~0.60 US\$/kWh (0.50 €/kWh) (central Europe) down to ~0.30 US\$/kWh (0.25 €/kWh) in regions of high solar irradiation. This electricity is generally fed into the electrical grid on the customer's side of the meter. The cost can be compared to prevailing retail electric pricing (as of 2005), which varied from between 0.04 and 0.50 US\$/kWh worldwide. (Note: in addition to solar irradiance profiles, these costs/kWh calculations will vary depending on assumptions for years of useful life of a system. Most c-Si panels are warranted for 25 years and should see 35+ years of useful life.)

3.2.7 Solar Cells and Energy Payback

The energy payback time, defined as the recovery time required for generating the energy spent for manufacturing a modern photovoltaic module is typically from 1 to 4 years^{[9][10]} depending on the module type and location. Generally, thin-film technologies - despite having comparatively low conversion efficiencies - achieve significantly shorter energy payback times than conventional systems (often < 1 year).^[11] With a typical lifetime of 20 to 30 years, this means that modern solar cells are net energy producers, i.e. they generate significantly more energy over their lifetime than the energy expended in producing them.^{[9][12][13]}

Crystalline silicon devices are approaching the theoretical limiting efficiency of 29%^[14] and achieve an energy payback period of 1–2 years.

3.3 System Performance

3.3.1 Insolation and Energy

At high noon on a cloudless day at the equator, the power of the sun is about 1 kW/m^2 on the Earth's surface, to a plane that is perpendicular to the sun's rays. As such, PV arrays can track the sun through each day to greatly enhance energy collection. However, tracking devices add cost, and require maintenance, so it is more common for PV arrays to have fixed mounts that tilt the array and face due South in the Northern Hemisphere (in the Southern Hemisphere, they should point due North). The tilt angle, from horizontal, can be varied for season, but if fixed, should be set to give optimal array output during the peak electrical demand portion of a typical year.

For the weather and latitudes of the United States and Europe, typical insolation ranges from $4 \text{ kWh/m}^2/\text{day}$ in northern climes to $6.5 \text{ kWh/m}^2/\text{day}$ in the sunniest regions. Typical solar panels have an average efficiency of 12%, with the best commercially available panels at 20%. Thus, a photovoltaic installation in the southern latitudes of Europe or the United States may expect to produce $1 \text{ kWh/m}^2/\text{day}$. A typical "150 watt" solar panel is about a square meter in size. Such a panel may be expected to produce 1 kWh every day, on average, after taking into account the weather and the latitude.

In the Sahara desert, with less cloud cover and a better solar angle, one could ideally obtain closer to $8.3 \text{ kWh/m}^2/\text{day}$ provided the nearly ever present wind would not blow sand on the units. The unpopulated area of the Sahara desert is over 9 million km^2 , which if covered with solar panels would provide 630 terawatts total power. The Earth's current energy consumption rate is around 13.5 TW at any given moment (including oil, gas, coal, nuclear, and hydroelectric).

3.3.2 Tracking the sun

Trackers and sensors to optimize the performance are often seen as optional, but tracking

systems can increase viable output by up to 100%. PV arrays that approach or exceed one megawatt often use solar trackers. Accounting for clouds, and the fact that most of the world is not on the equator, and that the sun sets in the evening, the correct measure of solar power is insolation – the average number of kilowatt-hours per square meter per day. For the weather and latitudes of the United States and Europe, typical insolation ranges from 4kWh/m²/day in northern climes to 6.5 kWh/m²/day in the sunniest regions.



Fig: 3-10 Sun tracker

For large systems, the energy gained by using tracking systems outweighs the added complexity (trackers can increase efficiency by 30% or more).

3.3.3 Shading and dirt Photovoltaic cell electrical output is extremely sensitive to shading. When even a small portion of a cell, module, or array is shaded, while the remainder

is in sunlight, the output falls dramatically due to internal 'short-circuiting' (the electrons reversing course through the shaded portion of the p-n junction).

If the current drawn from the series string of cells is no greater than the current that can be produced by the shaded cell, the current (and so power) developed by the string is limited. If enough voltage is available from the rest of the cells in a string, current will be forced through the cell by breaking down the junction in the shaded portion. This breakdown voltage in common cells is between 10 and 30 volts. Instead of adding to the power produced by the panel, the shaded cell absorbs power, turning it into heat. Since the reverse voltage of a shaded cell is much greater than the forward voltage of an illuminated cell, one shaded cell can absorb the power of many other cells in the string, disproportionately affecting panel output. For example, a shaded cell may drop 8 volts, instead of adding 0.5 volts, at a particular current level, thereby absorbing the power produced by 16 other cells.^[10] Therefore it is extremely important that a PV installation is not shaded at all by trees, architectural features, flag poles, or other obstructions.

Most modules have bypass diodes between each cell or string of cells that minimize the effects of shading and only lose the power of the shaded portion of the array (The main job of the bypass diode is to eliminate hot spots that form on cells that can cause further damage to the array, and cause fires.).

Sunlight can be absorbed by dust, snow, or other impurities at the surface of the module. This can cut down the amount of light that actually strikes the cells by as much as half. Maintaining a clean module surface will increase output performance over the life of the module.

3.3.4 Temperature

Module output and life are also degraded by increased temperature. Allowing ambient air to flow over, and if possible behind, PV modules reduces this problem.

3.3.5 Module efficiency

In 2010, solar panels available for consumers can have a yield of up to 19%,^[11] while commercially available panels can go as far as 27%.^[12] Thus, a photovoltaic installation in the southern latitudes of Europe or the United States may expect to produce 1 kWh/m²/day. A typical "150 watt" solar panel is about a square meter in size. Such a panel may be expected to produce 1 kWh every day, on average, after taking into account the weather and the latitude.

3.3.6 Monitoring

Photovoltaic systems need to be monitored to detect breakdown and optimize their operation. Several **photovoltaic monitoring** strategies depending on the output of the installation and its nature. Monitoring can be performed on site or remotely. It can measure production only, retrieve all the data from the inverter or retrieve all of the data from the communicating equipment (probes, meters, etc.). Monitoring tools can be dedicated to supervision only or offer additional functions. Individual inverters may include monitoring using manufacturer specific protocols and software. Energy metering of an inverter may be of limited accuracy and not suitable for revenue metering purposes. A third-party data acquisition system can monitor multiple inverters, using the inverter manufacturer's protocols , and also acquire weather-related information. Independent smart meters may measure the total energy production of a PV array system. Separate measures such as satellite image analysis or a solar radiation meter (a pyranometer) can be used to estimate total insolation.

Data collected from a monitoring system can be displayed remotely over the World Wide Web. Some companies offer analysis software to analyze system performance. Small residential systems may have minimal data analysis requirements other than perhaps total energy production; larger grid-connected power plants can benefit from more detailed investigations of performance.

3.3.7 Performance factors

Uncertainties in revenue over time relate mostly to the evaluation of the solar resource and to

the performance of the system itself. In the best of cases, uncertainties are typically 4% for year-to-year climate variability, 5% for solar resource estimation (in a horizontal plane), 3% for estimation of irradiation in the plane of the array, 3% for power rating of modules, 2% for losses due to dirt and soiling, 1.5% for losses due to snow, and 5% for other sources of error. Identifying and reacting to manageable losses is critical for revenue and O&M efficiency. Monitoring of array performance may be part of contractual agreements between the array owner, the builder, and the utility purchasing the energy produced.

Access to the Internet has allowed a further improvement in energy monitoring and communication. Dedicated systems are available from a number of vendors. For solar PV system that use micro Inverters (panel-level DC to AC conversion), module power data is automatically provided. Some systems allow setting performance alerts that trigger phone/email/text warnings when limits are reached. These solutions provide data for the system owner and the installer. Installers are able to remotely monitor multiple installations, and see at-a-glance the status of their entire installed base.

3.3.8 Module life

Effective module lives are typically 25 years or more.

3.3.9 Components

3.3.9.1 Trackers

A solar tracker tilts a solar panel throughout the day. Depending on the type of tracking system, the panel is either aimed directly at the sun or the brightest area of a partly clouded sky. Trackers greatly enhance early morning and late afternoon performance, substantially increasing the total amount of power produced by a system.

Trackers are effective in regions that receive a large portion of sunlight directly. In diffuse light (i.e. under cloud or fog), tracking has little or no value. Because most concentrated photovoltaic systems are very sensitive to the sunlight's angle, tracking systems allow them to produce useful power for more than a brief period each day.

Tracking systems improve performance for two main reasons. First, when a solar panel is perpendicular to the sunlight, the light it receives is more intense than it would be if angled. Second, direct light is used more efficiently than angled light. Special Anti-reflective coatings can improve solar panel efficiency for direct and angled light, somewhat reducing the benefit of tracking.

3.3.9.2 Inverters



Fig: 3-11. Inverter for grid connected PV

On the AC side, these inverters must supply electricity in sinusoidal form, synchronized to the grid frequency, limit feed in voltage to no higher than the grid voltage including disconnecting from the grid if the grid voltage is turned off.

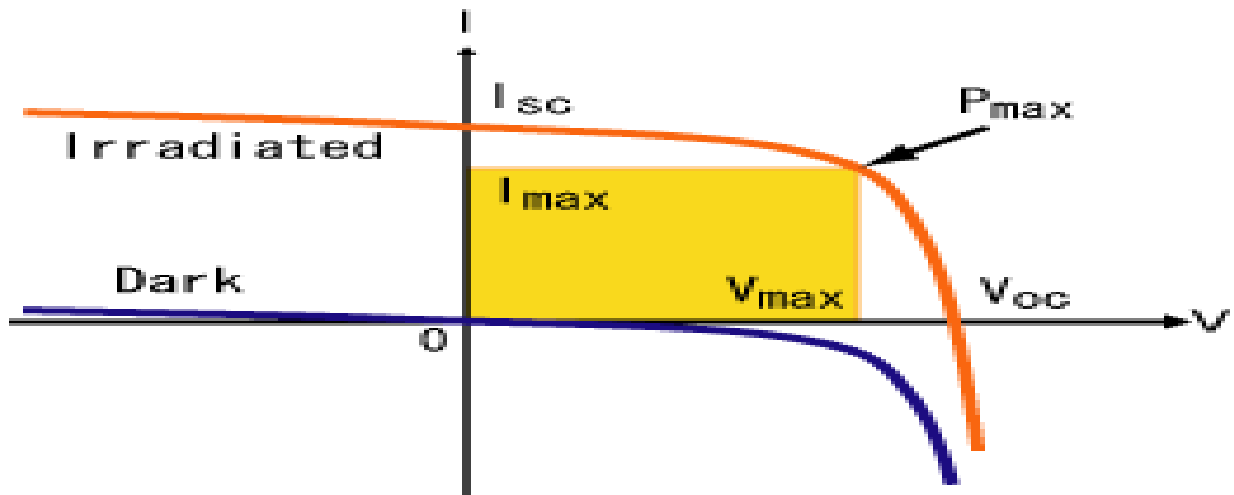


Fig: 3-12. I-V characteristics curve

On the DC side, the power output of a module varies as a function of the voltage in a way that power generation can be optimized by varying the system voltage to find the 'maximum power point'. Most inverters therefore incorporate 'maximum power point tracking'.

A solar inverter may connect to a string of solar panels. In small installations a solar micro-inverter is connected at each solar panel.

For safety reasons a circuit breaker is provided both on the AC and DC side to enable maintenance. AC output may be connected through an electricity meter into the public grid.

The meter must be able to run in both directions.

In some countries, for installations over 30kWp a frequency and a voltage monitor with disconnection of all phases is required.

CHAPTER 4

MODELING OF THIN FILM SOLAR CELL

4.1 Modeling Parameters

The model of thin film heterojunction solar cell module has to take into account electrical, optical and geometrical parameters [16]. Light is absorbed in the solar cell and a current is generated following the diode equation. There is absorption of light in the transparent front contact which leads to optical losses. Major electrical series and shunt resistance of thin film heterojunction solar cell module are indicated in fig-6. we are considering heterojunction solar cell in the following fig where the p-type is CIGS and n-type is Buffer/ZnO. The lateral current in the transparent front contact (ZnO:Al) and back contact (Mo) is not uniform, enhance these layer constitute distributed series resistance $R_{ZnO:Al1}$, $R_{ZnO:Al2}$ etc for ZnO:Al and R_{Mo1} , R_{Mo2} etc for Mo. There is also a discrete series resistance R_d . There is an additional resistance R_c at the ZnO:Al/Mo contact. The CIGS layer provides a shunting path between the front contact and the back contact indicated by R_{sh1} , R_{sh2} etc.

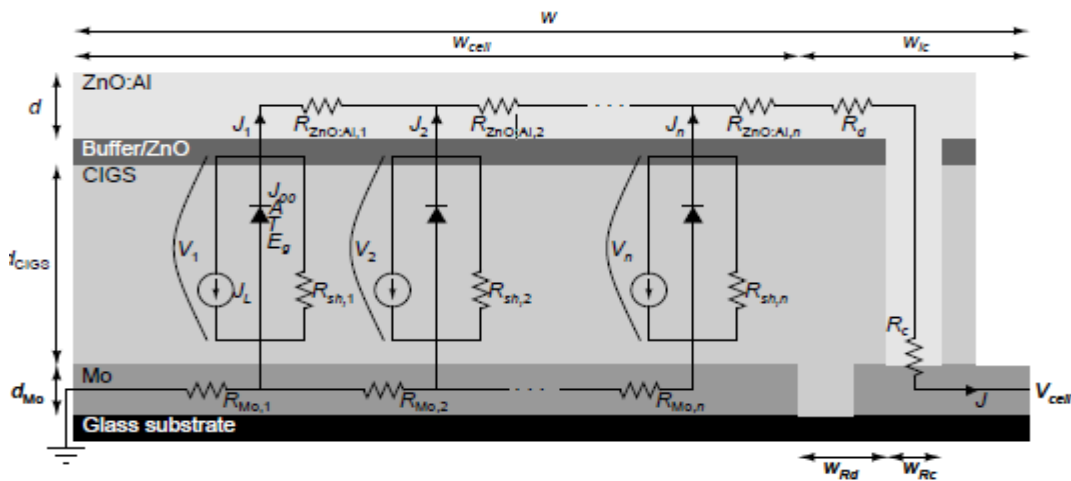


Fig: 4-1. Equivalent circuit of heterojunction solar cell

4.1.1 CIGS Absorber

P-type CIGS absorber has a high concentration of holes and low concentration of electron, hence holes flow readily through the p-type material [17]. The opposite is true for n-type material. The excess electron-hole pairs are generated by the light that is absorbed in the CIGS layer. The asymmetrical properties of the heterojunction encourage a flow of generated holes to the back contacts and a flow of generated electron to the n-type material. Therefore, an illuminated heterojunction which is electrically shorted will cause a net current flow. In the model, the current is generated in each lateral point of the active cell, according to the diode equation.

$$J_i = J_0 e^{qv_i / AkT} - J_L$$

$$J_0 = J_{00} e^{-E_g / AkT}$$

Where $i=1,2,3,\dots,n$

The light generated current J_L depends on the transmission of incident through the transparent front contact as

$$J_L = T_{Zno:Al} J_{L,in}$$

Where $T_{Zno:Al}$ is a function of transmittance of the incident light through the ZnO:Al and $J_{L, in}$ is the incident light generated current. The incident light generated current has a typical value about 350 A/m^2 at STC.

4.1.2 Transparent Front Contact

The following relationship holds for the sheet resistance, conductivity and thickness of ZnO:Al layer.

$$\text{Sheet resistance, } R_{s,Zno:Al} = 1/d\sigma_{Zno:Al}$$

Transmittance of light is a vital parameter to increase the efficiency of a thin film solar cell. We are going to discuss about this parameter.

4.1.3 Transmission of Light

The optical transmission of the incident light through the transparent front contact decreases sharply when the ZnO:Al layer becomes thicker and as a result has less sheet resistance. A model that describes the transmittance, $T_{\text{Zno:Al}}$, as a function of sheet resistance is [16]

$$T_{\text{Zno:Al}} = T_1 - (R_1 / R_{\text{Zno:Al}})^{m_1}$$

Experiments have been performed to determine the transmission through the ZnO:Al layer as a function of sheet resistance at solarex corporation [18], at Uppasala University [19] in the present study. The fitting parameters are $T_1=1$, $R_1=0.3707$ ohm and $m_1=0.8226$ [19]. Thus we get the complete equation as following

$$T_{\text{Zno:Al}} = 1 - (0.3707 / R_{\text{Zno:Al}})^{0.8226}$$

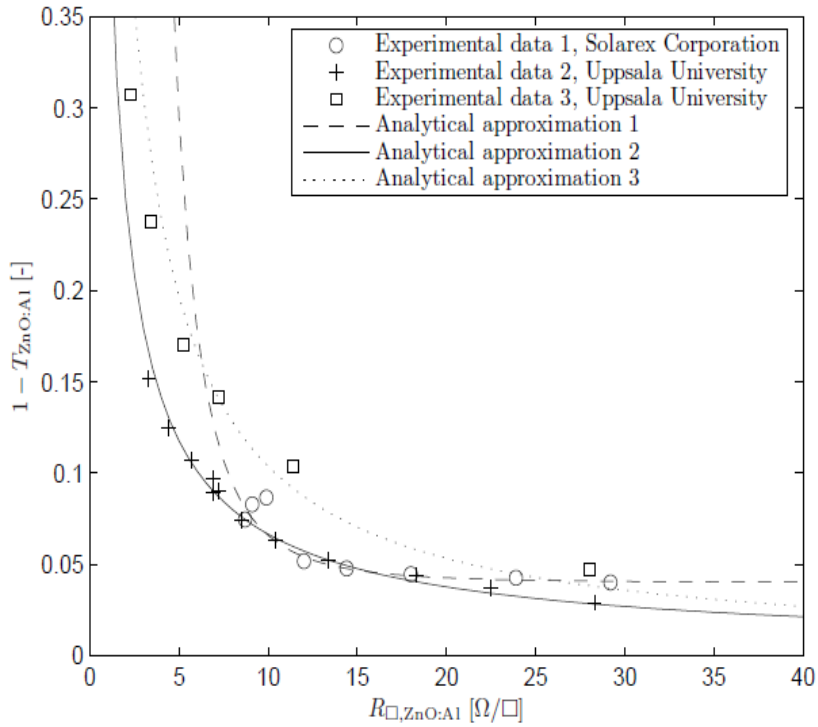


Fig: 4-2. Transmittance of ZnO:Al layer as a function of sheet resistance

We can also deduce some of the relationship between the efficiency of solar cell and transmittance parameter. These relationship curves are also varied with the cell width. In the following we are giving these relationship.

Cell width(mm)	Relationship
5	E=5-131.4T+568.8T²-993.3T³+784.7T⁴-233.6T⁵
7	E=6-27.2T+40.5T²-19.3T³
9	E=6-61.6T+218.3T²-356.5T³+277.5T⁴-83.7T⁵

Where E= efficiency, T=transmittance

4.1.4 Back Contact

The thickness of Mo layer is typically 0.5 μm and sheet resistance is about 0.65ohm[12].The conductivity of Mo can be calculated as 3.1E6 S/m.

4.1.5 Bandgap and Carrier Lifetime

Bandgap and carrier lifetime are interrelated parameters for solar cell efficiency. Later we will see the relationship between these two parameters in the curve. It is seen that the efficiency varies with the carrier recombination lifetime where bandgap energy works as an effective parameter. We can get different relationship between the efficiency and carrier recombination lifetime for different bandgap.

Energy Gap(eV)	Relationship
1.7360	$E=4+5.7X-0.4X^2+0.0038X^3+3.4E-6X^4$
1.5522	$E=6+4.9X-0.24X^2+0.0022X^3-1.99E-6X^4$
1.4845	$E=7+3.06X-0.03X^2+6.15E-5X^3-3.15E-8X^4$

4.1.6 Cell Width

Cell width has a strong influence on the efficiency of solar cell. As we know that the efficiency can also be indicated by fill factor (FF), so it is very easy to realize that the cell width has a great influence on the fill factor of a solar cell. With a certain range of cell width[20], we got a relationship between the fill factor (FF) and cell width. The relation can be expressed as –

$$FF=0.16+0.095W-0.0037W^2$$

Where FF=fill factor

W=cell width

4.1.7 Effect of Carrier Mobility on Efficiency-cell Width Relation

Next we will see in the simulated curves that there is great effect of carrier mobility on the efficiency vs base width curve. It is found that when the mobility of the carrier changes, the characteristics of the relationship also changes.

From the simulation, when the mobility is below the $15.714 \text{ cm}^2/v_s$ [21], the efficiency decreases with the increase of specific range of base width. But when take the value of mobility beyond $15.714 \text{ cm}^2/v_s$, the efficiency increases with the increase of base width. These all relationships are found and given below-

Mobility(cm^2/v_s)	Relationship(Efficiency-Base width)
10	$E=0.15+8.5W-0.81W^2$
15.1428	$E=0.15+9.19W-0.83W^2$
15.4280	$E=0.2+9.22W-0.8W^2$
15.7142	$E=1+8.3W-0.7W^2$
100	$E=10-0.14W+0.14W^2$
1000	$E=15+0.12W+0.15W^2$

Where E= Efficiency , W= Base width in μm .

4.1.8 Temperature Effect

Our study is related to different parameter which make influence on the efficiency of a solar cell. Temperature of a solar cell is such a parameter that can change the shape of the fill factor curve. We will see later that when there is an increase of temperature in solar cell, the fill factor also increase little bit. But after a certain temperature, it goes down sharply. A relationship between the fill factor-temperature can be found an expressed as following-

$$FF=0.75+2.8E-6T+3.9E-5T^2-1.67E-6T^3+1.4E-8T^4$$

Where T=Temperature

FF= Fill factor

We have to model a solar cell in such a way that must not cross that temperature (250C) from which the fill factor curve goes drastically fallen down. So, we must have cooling system in modern design solar cell.

CHAPTER 5

SIMULATION, RESULTS AND DISCUSSION

5.1. Parameters Adjustment

The parameters in the model are set to fit measured data of actual model. The parameter are set, so that the simulated curve and measured curve match each other.

As there are a lot of parameter, we are interested to give an overview some of them like cell width, mobility of the carrier, bandgap energy, carrier recombination life time, temperature, transmittance in the front contact etc. For different value of all these parameters, the shape of the curve get changed. Slowly we will discuss the optimal point for all of these parameters later.

Here we can see that the parameter are set so that the measured curve and simulated curve match each other. Some input parameters are given, some are measured and some have to be adjusted.

We have tried to adjust all of these parameters that match with the actual module of the solar cell.

5.2 Transmittance Optimization

Simulation are performed to investigate how the sheet resistance of the ZnO:Al influences the efficiency of heterojunction thin film solar cell module. For each investigated cell width the thickness of the ZnO:Al layer, d is varied. Since d is varied, sheet resistance also changes when the thickness increases, the sheet resistance would be lower and the optical transmission of the incident light $T_{\text{ZnO:Al}}$ sharply decreases. So as the transmittance is varied it also changes the efficiency of the solar cell.

Fig-5.1 shows the module efficiency at different values of transmittance of light. The simulation were performed for modules with cell width of 3mm, 7mm and 9mm.

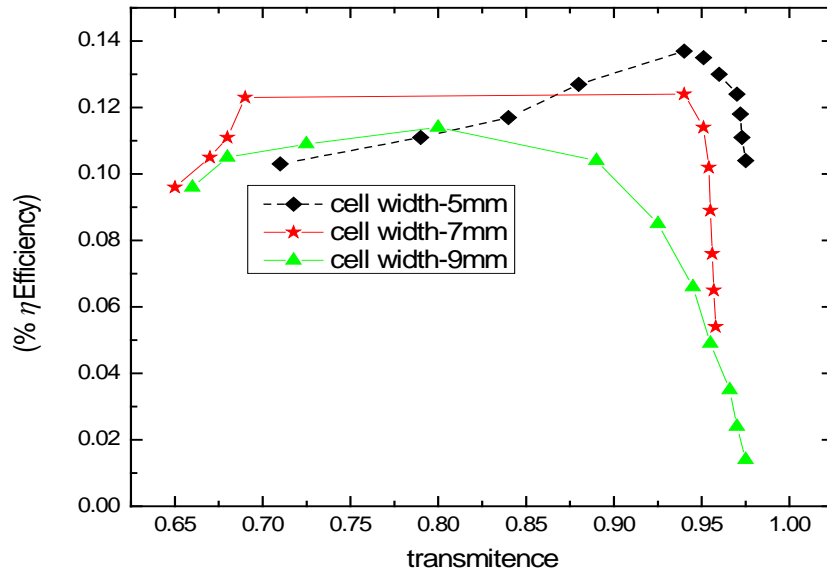


Fig-5.1. Simulation showing module efficiency at different transmittance. Three different approximations describe the cell width of the solar cell.

The first conclusion is that the maximum efficiency increases with decreasing cell width. If the shape of the four curves are compared then it is easy to see that when the cell width is 5mm, the efficiency of solar cell is highest at a certain transmittance. But when cell width increases, the height of the curve decreases and maximum efficiency for the 7mm and 9mm cell width at a certain transmittance point is lower respectively than the 5mm cell width solar cell.

It is also seen that the curves become flattered around its maximum value with decreasing cell width. It is observed that for 5mm cell width when the transmittance is 0.94 then the efficiency is around 13.7%. But it decreases for 7mm cell width become 12.3% at 0.69 transmittance. Similarly when cell width is 9mm, efficiency becomes 11.4% at 0.8.

5.3 Recombination Lifetime Optimization

Simulations are carried out to investigate the performance of heterojunction thin film solar cell. The optimal relationship between the carrier recombination lifetime and the efficiency of a solar cell is simulated for different bandgap energy. Carrier recombination lifetime has a major influence on conversion efficiency where the mitigation of non-radiative process is highly important.

Here we have considered the thin film intermediate band solar cell (IBSC) which is made of oxygen-doped ZnTe. The dependence of IBSC conversion efficiency on minority carrier lifetime and intermediate bandgap position is depicted in fig-5.2, From the simulated curve we can see, the optimal position of the carrier recombination life time τ have a dependence on the bandgap energy.

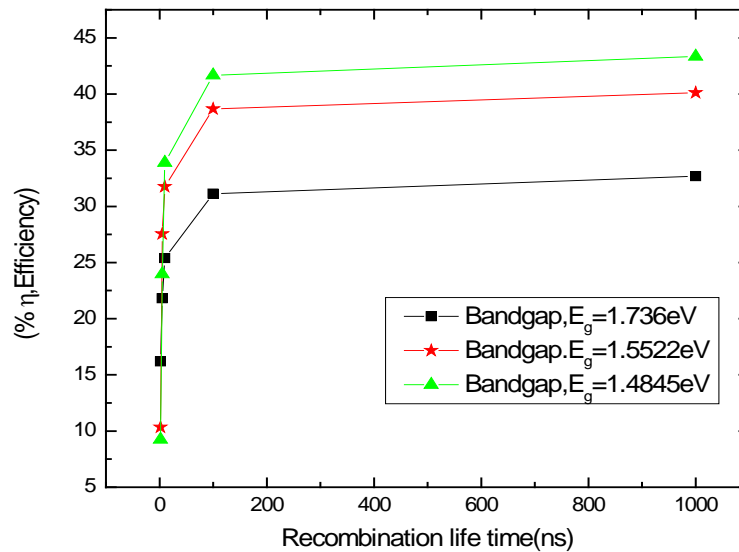


Fig-5.2. Simulation showing module efficiency at different recombination life time. Three different bandgap energy influences on the shape of the curve.

The first conclusion from the simulated curve is achieved that the efficiency of solar cell becomes saturated after a specific value of carrier recombination lifetime. This occurs at a

certain value of bandgap energy. We can also see from the curve that when we vary the band gap energy level of semiconductors, the efficiency of solar cell also varies. It is observed that at a specific bandgap of 1.736eV, we can get the efficiency around 31.14 %, When the carrier recombination lifetime $\tau=2\text{ns}$. After that it gets saturated. Efficiency does not increase further though we increase the recombination lifetime. This simulation has been done for three bandgap materials. Every time it is found that increasing the bandgap results decreasing the efficiency of the solar cell.

5.4 Temperature Optimization

Simulation is done to investigate the performance of thin film solar cell at different temperatures. In fig-5.3, the efficiency is plotted as a function of temperature of solar cell.

Temperature is an important parameter which we can make influence on the shape of the fill factor curve of solar cell. From the simulated curve, it is seen that at a given range of temperature, the fill factor at first rises with the increase of temperature. But there is also an inverse relationship between the fill factor and temperature in the simulation on curve after a certain temperature.

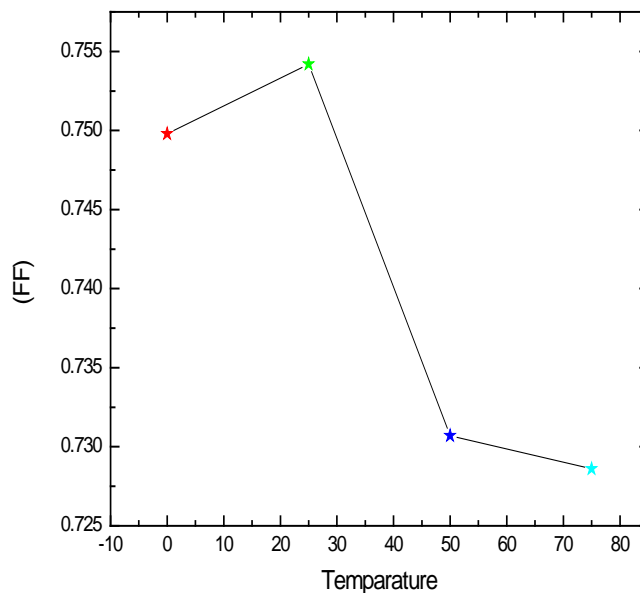


Fig-5.3. Simulation showing module efficiency at different temperatures.

Now we can make a conclusion from the simulation curves. First conclusion is that when there is an increase of temperature, the fill factor of solar cell increases. But this does not continue further. We can see from the shape of the curve that slowly raise of temperature makes a slow increase of fill factor. But a certain limit of temperature, there is a sharp degradation of the solar cell fill factor.

When the temperature is from (0°C to 25°C), the fill factor increases slowly around 0.75 to 0.7542. But when the temperature range increases further, the fill factor decreases sharply from 0.7542 to 0.7307. We can conclude that after 25°C . There is a drastic fall down of fill factor of solar cell, so we have to maintain this temperature point for higher efficiency of solar cell.

5.5 Cell Width Optimization

The dependence of power conversion efficiency on base width of ZnTeO ($E_g=2.3\text{eV}$, $E_i=1.8\text{eV}$) is shown in fig-5.4 Simulated curves shows the efficiency η of modules with different base width at different mobility of the carrier.

The (IBSC) device structure under study will have a strong dependence on the base width of solar cell as well as on the carrier transport where photogenerated carriers in the depletion region will need to drift to the n -and p-contact prior to recombination. So, the carrier mobility will therefore be a crucial parameter for this device. We will see that for a fixed mobility of carrier when we vary the base width, the efficiency will also vary.

From the simulated curve, we see when the mobility is $10\text{ cm}^2/\text{vs}$, the efficiency is higher at $1\text{ }\mu\text{m}$ base width than $10\text{ }\mu\text{m}$ base width. This phenomenon continues for a certain value of mobility of the carrier. When the mobility reaches at $15.7142\text{ cm}^2/\text{vs}$, we see that the pattern of the efficiency curve changes. From this value of carrier mobility, the efficiency increases with the increase of base width. We see that when the mobility is $10\text{ cm}^2/\text{vs}$, $15.1428\text{ cm}^2/\text{vs}$ and $15.428\text{ cm}^2/\text{vs}$, the efficiency vs base width has a downwards sloping curves. But for $15.7142\text{ cm}^2/\text{vs}$, $100\text{ cm}^2/\text{vs}$ and $1000\text{ cm}^2/\text{vs}$, the curve becomes upward sloping. So, here we

have drawn a conclusion that for a ZnTeO thin film solar cell for certain value of mobility of the carrier, the pattern of the efficiency curve got changed.

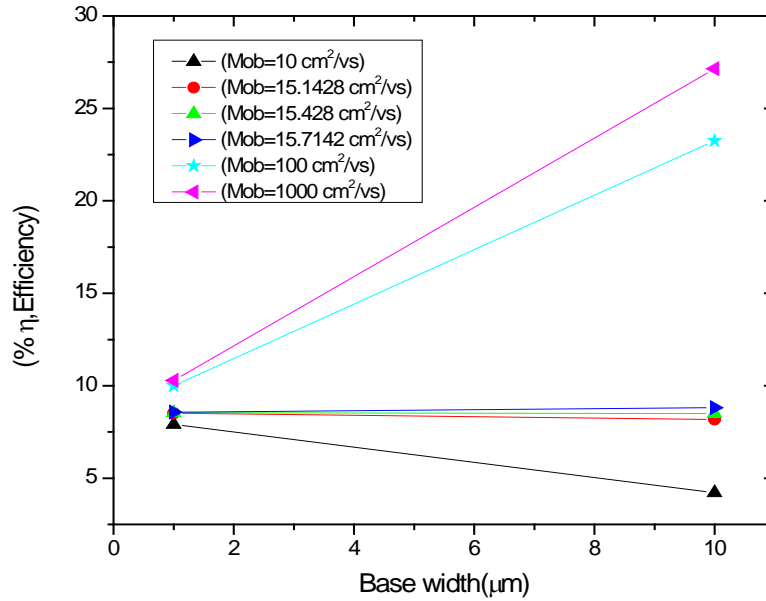


Fig-5.4. Simulation showing module efficiency at different base width. At different values of carrier mobility, the pattern of the curve has changed.

Findings of this Work (Mobility Optimization)

In above, we have already discussed about the effect of carrier mobility in the efficiency vs base-width curve. From the simulated curve, we have some findings about this relationship. For ZnTeO thin film solar cell, we see that when the carrier mobility reaches 15.7142 cm²/vs, the efficiency of solar cell increases with the increase of specific range of base width. So, we can say that if we ensure that the mobility of the carrier is about 15.7142 cm²/vs or above then we can get higher efficiency from the solar cell by increasing the base width in a specific range. But below 15.7142 cm²/vs mobility, we see the vice versa relation. So a designer should check at first this optimal value of carrier mobility and then he should fix the base width of the solar cell for higher efficiency.

5.6 Fill Factor-Cell Width Relation

We have simulated the relationship between the fill factor and cell width in the following curve. As previously discussed that the cell width is an important parameter for solar cell, so it has been tried to find the relationship between this two terms.

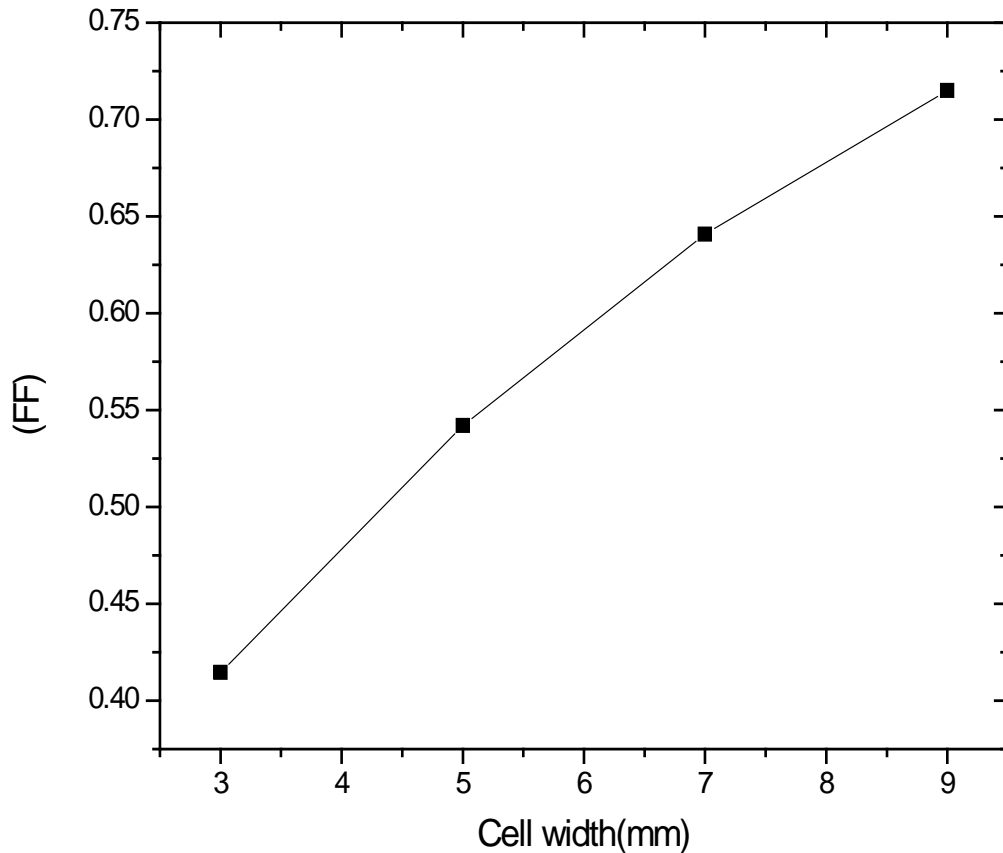


Fig-5.5. Variation of fill factor (FF) with cell width of a given range (3mm-9mm)

Here we have simulated the curve at a given range of cell width. This is a clear indication that within this range of cell width the fill factor increases. But there must be an optimal value of cell width at which the fill factor has its highest value. After this cell width if we increase it, the fill factor will go down. So, a designer must take it into account.

CHAPTER 6

CONCLUSION AND SUGGESTION

6.1 Conclusion

“Solar energy is free and available in all over the world but we have to collect it with high efficiency”- This term made the researchers working on this renewable energy. The rationale of this thesis was to investigate the improvement of efficiency of thin film Solar cell. A study has been carried out so far, to find the parameters for which the efficiency of a solar cell varies. On the foregoing process, it was found that some of the parameters have strong influence on the efficiency of the solar cell. Parameters like bandgap energy, carrier recombination lifetime, transmittance, temperature, cell width, mobility etc are found and it has been demonstrated to work on the efficiency improvement by varying these parameters.

Further study has been carried about these parameters from different references and established the relationship between them. For this, some simulation with the help of various software has been done and different curves were generated. From these curves, the optimal operating point for different parameters, at which solar cell has its maximum efficiency, has been performed.

6.2 Suggestion for Future Works

The further unvestigation will bear some objective like-

- ❖ The change of the behavior of efficincy for different parameters is discussed so far is related to CIGS and ZnTeO thinfilm solar cell. In further investigation, the thesis will help to find the change of efficiency that occurs for other different type of solar cell like organic solar cell, ***** silicon etc.
- ❖ Other important parameter also has to find out in future which ha

REFERENCES

- [1] Alfred Smee (1849). Elements of electro-biology, or the voltaic mechanism of man; of electro-pathology, especially of the nervous system; and of electro-therapeutics. London: Longman, Brown, Green, and Longmans.
- [2] "The Nobel Prize in Physics 1921: Albert Einstein", Nobel Prize official page
- [3] "Light sensitive device" U.S. Patent 2,402,662 Issue date: June 1946
- [4] K. A. Tsokos, "Physics for the IB Diploma", Fifth edition, Cambridge University Press, Cambridge, 2008, ISBN 0521708206
- [5] Perlin, John (2004). "The Silicon Solar Cell Turns 50". National Renewable Energy Laboratory. Retrieved 5 October 2010.
- [6] Perlin, John. *From Space to Earth: The Story of Solar Electricity*. Harvard University Press, 2002, pg. 53
- [7] John Perlin, "From Space to Earth: The Story of Solar Electricity", Harvard University Press, 2002, pg. 54
- [8] \$1/W Photovoltaic Systems DOE whitepaper August 2010
- [9] <http://247wallst.com/2011/10/06/solar-stocks-does-the-punishment-fit-the-crime-fslr-spwra-stp-jaso-tsl-ldk-tan/>
- [10] NASA Solar System Exploration - Sun: Facts & Figures retrieved 27 April 2011 "Effective Temperature ... 5777 K"
- [11] Antonio Luque and Steven Hegedus (2003). *Handbook of Photovoltaic Science and Engineering*. John Wiley and Sons. ISBN 0471491969.
- [12] 12 People building their own solar systems from kits
- [13] 13 Example of diy PV system with pictures
- [14] 14 Low-cost PV solar kit preferred by diy-communities
- [15] 15 VillageEarth AT SourceBook: PV-solar systems (info for diy-set ups)
- [16] M.BURGELMAN AND A.NIEMEGEREERS, *calculation of cis and CdTe module efficiency,1998*
- [17] M.GREEN Solar Cells-*Operating principle, Technology and system application*,The University of New South Wales,Kingston,1992
- [18] S.WIELDMAN, J.KESSLER, L.RUSSEL, J.FROGLEBOCH, S.SKIBO, T.LOMMANSON, D.CARLSON AND R. ARYA, proc. 13 th European photovoltaic Solar Energy Conference, Nice, 1995,H.S Stephens & Associates,1995, pp.2059-2062
- [19] J. WENNERBERG, J.KESSLER AND L.STOLT, Technical Digest of the International PVSEC-11, sapporo,Hokkaido,Japan,pp.827-828
- [20] JOHN JOHNSON, *Modelling and Optimization of CIGS Solar cell Module Master's Thesis 2007*